nature aging

ARTICLES

https://doi.org/10.1038/s43587-021-00070-2

Check for updates

ADAMANT: a placebo-controlled randomized phase 2 study of AADvac1, an active immunotherapy against pathological tau in Alzheimer's disease

Petr Novak[1]✉, Branislav Kovacech[2], Stanislav Katina[1], Reinhold Schmidt[3], Philip Scheltens[4], Eva Kontsekova[2], Stefan Ropele[5], Lubica Fialova[2], Milica Kramberger[6], Natalia Paulenka-Ivanovova[2], Miroslav Smisek[1], Jozef Hanes[2], Eva Stevens[2], Andrej Kovac[2], Stanislav Sutovsky[7], Vojtech Parrak[2], Peter Koson[1], Michal Prcina[2], Jaroslav Galba[2], Martin Cente[2], Tomas Hromadka[8], Peter Filipcik[2], Juraj Piestansky[2], Maria Samcova[1], Carmen Prenn-Gologranc[1], Roman Sivak[1], Lutz Froelich[9], Michal Fresser[10], Martin Rakusa[11], John Harrison[4], Jakub Hort[12], Markus Otto[13], Duygu Tosun[14], Matej Ondrus[1], Bengt Winblad[15,16], Michal Novak[10] and Norbert Zilka[2]

Alzheimer's disease (AD) pathology is partly characterized by accumulation of aberrant forms of tau protein. Here we report the results of ADAMANT, a 24-month double-blinded, parallel-arm, randomized phase 2 multicenter placebo-controlled trial of AADvac1, an active peptide vaccine designed to target pathological tau in AD (EudraCT 2015-000630-30). Eleven doses of AADvac1 were administered to patients with mild AD dementia at 40 μg per dose over the course of the trial. The primary objective was to evaluate the safety and tolerability of long-term AADvac1 treatment. The secondary objectives were to evaluate immunogenicity and efficacy of AADvac1 treatment in slowing cognitive and functional decline. A total of 196 patients were randomized 3:2 between AADvac1 and placebo. AADvac1 was safe and well tolerated (AADvac1 $n = 117$, placebo $n = 79$; serious adverse events observed in 17.1% of AADvac1-treated individuals and 24.1% of placebo-treated individuals; adverse events observed in 84.6% of AADvac1-treated individuals and 81.0% of placebo-treated individuals). The vaccine induced high levels of IgG antibodies. No significant effects were found in cognitive and functional tests on the whole study sample (Clinical Dementia Rating-Sum of the Boxes scale adjusted mean point difference −0.360 (95% CI −1.306, 0.589)), custom cognitive battery adjusted mean *z*-score difference of 0.0008 (95% CI −0.169, 0.172). We also present results from exploratory and post hoc analyses looking at relevant biomarkers and clinical outcomes in specific subgroups. Our results show that AADvac1 is safe and immunogenic, but larger stratified studies are needed to better evaluate its potential clinical efficacy and impact on disease biomarkers.

The neuropathological hallmarks of AD are the deposition of amyloid-β and aggregation of tau protein[1–3]. Neurofibrillary tau pathology is closely tied to key aspects of the neurodegenerative process. The distribution and quantity of neurofibrillary lesions is strongly correlated with both the severity and pattern of brain atrophy[4] and with the clinical phenotype and severity of cognitive impairment and dementia[5,6]. The deposition pattern of neurofibrillary pathology, as seen by tau positron emission tomography (PET), is also predictive of future brain atrophy[7] and longitudinal cognitive decline[8].

According to current understanding, following seminal events in the entorhinal cortex and/or brainstem[9], the neurons that initially develop neurofibrillary lesions begin to shed seeding-capable tau aggregates that bear similarities to prions. Subsequently, tau pathology propagates through the brain along neuronal pathways[10] as the tau seeds produced by affected neurons enter healthy but vulnerable cells, where they sequester and convert physiological tau via template-mediated conformational change[11]. Neuronal damage occurs via a combination of loss of function and toxic gain of function of tau[12].

[1]AXON Neuroscience CRM Services SE, Bratislava, Slovakia. [2]AXON Neuroscience R&D Services SE, Bratislava, Slovakia. [3]Clinical Division of Neurogeriatrics, Department of Neurology, Medical University Graz, Graz, Austria. [4]Alzheimer Center, Amsterdam University Medical Centers, Amsterdam, the Netherlands. [5]Clinical Division of General Neurology, Department of Neurology, Medical University Graz, Graz, Austria. [6]Department of Neurology, University Medical Centre Ljubljana, Ljubljana, Slovenia. [7]1st Department of Neurology, Faculty of Medicine, Comenius University and University Hospital, Bratislava, Slovakia. [8]Institute of Neuroimmunology, Slovak Academy of Sciences, Bratislava, Slovakia. [9]Department of Geriatric Psychiatry, Zentralinstitut für Seelische Gesundheit, Medical Faculty Mannheim University of Heidelberg, Heidelberg, Germany. [10]AXON Neuroscience SE, Larnaca, Cyprus. [11]Department of Neurological Diseases, University Medical Centre Maribor, Maribor, Slovenia. [12]Memory Clinic, Department of Neurology, Charles University, 2nd Faculty of Medicine and Motol University Hospital, Prague, Czech Republic. [13]Department of Neurology, Ulm University Hospital, Ulm, Germany. [14]Department of Radiology and Biomedical Imaging, University of California, San Francisco, CA, USA. [15]Division of Neurogeriatrics, Center for Alzheimer Research, Karolinska Institutet, Solna, Sweden. [16]Theme Inflammation and Aging, Karolinska University Hospital, Huddinge, Sweden. ✉e-mail: petr.novak@axon-neuroscience.eu

There is a growing body of evidence showing that aggregated tau, either in free form or in exosomes, can be transferred from donor cells (either neurons or glial cells) to recipient cells using various routes, including receptor-mediated (heparan sulfate proteoglycans, LDL-receptor-related protein 1)[13,14] or nonreceptor-mediated endocytosis/micropinocytosis or transport via nanotubes (in vitro data)[15]. The identification of extracellular pathological tau and its ability to spread in a prion-like fashion have modified the strategy of immunotherapy toward targeting the pathological tau located in the extracellular space[16]. Extracellular tau is a crucial part in this propagation of tau pathology and at the same time is more readily accessible to drugs than its intracellular counterpart, thus constituting an excellent treatment target. As the rate of disease progression depends upon the level of seeding-capable 'tauons' in the brain and their interneuronal transfer[17], it follows that reducing their amount and obstructing their entry into healthy neurons should slow or even halt the propagation of neurofibrillary degeneration. Tau encapsulated in extracellular vesicles is less likely to be accessible for immunotherapy and can still spread tau pathology; however, to a much lesser extent compared to free tau[18].

Vaccines and humanized antibodies in clinical development target a range of extracellular tau species, with some being aimed at the amino- or carboxy-terminus and others binding the proline-rich region or microtubule-binding repeat domain of tau[19,20]. Active immunotherapy has several desirable properties that make it a suitable candidate for reducing the amount of neurofibrillary degeneration in the brain: it does not elicit inactivating anti-drug antibodies that are the bane of various passive immunotherapy products[21], it is cost effective, easy to administer and ultimately, a feasible candidate for primary prevention.

We previously identified amino acid sequences in the microtubule-binding region of tau protein that are essential for pathological tau–tau interaction and aggregation, consisting of four highly homologous and yet independent binding regions on tau, each of which behaves as a separate epitope. The X-ray structure indicates that the four epitopes form protruding structures on the tau molecule. Targeting them via the monoclonal antibody DC8E8 resulted in effective inhibition of tau aggregation[22], prevented neuronal uptake of tau seeds and promoted the microglial clearance of extracellular pathological tau[23,24].

The DC8E8 antibody epitopes served as a template in the development of AADvac1, an active immunotherapy targeting a pathological conformation of tau protein found in AD and various tauopathies. We have shown that AADvac1 reduces the amount of neurofibrillary pathology in tau-transgenic rats and improves their moribund phenotype[25]. In humans, AADvac1 treatment leads to high IgG response rates also in elderly patients with AD. The induced antibodies display a manifold higher affinity for pathological over healthy tau and are reactive with all investigated types of tau pathology, including neurofibrillary lesions in human AD, Pick's disease, corticobasal degeneration and progressive supranuclear palsy. In phase 1 studies, the safety profile of AADvac1 was benign; encouraging signals were observed on MRI volumetry and cognitive assessments[26,27].

Based on the above, AADvac1 was advanced into phase 2 development, with the aim of primarily testing safety and immunogenicity in a larger cohort of patients with AD in the ADAMANT (Alzheimer's Disease Active immunization and disease Modification by AXON Neuroscience directed against Tau) trial.

Results

Patient characteristics and analysis sets. A total of 196 patients with a diagnosis of mild AD supported by MRI and/or cerebral spinal fluid (CSF) biomarkers were enrolled between 16 June 2016 and 30 May 2017 and randomized in a 3:2 ratio to AADvac1 ($n=117$) or placebo ($n=79$). The last safety follow-up visit was on 25 June 2019.

The safety set comprised 196 patients who received at least one dose of AADvac1 or placebo and had at least one post-baseline safety assessment; this set was used for safety analyses. The full analysis set (FAS) comprised 193 patients who had at least one post-baseline efficacy assessment. Altogether, 163 FAS patients completed the study via attending the end-of-study visit at week 104; this was the primary set for efficacy analyses. The attrition rate between the safety set and the set of study completers was 16.8%, with 14.5% dropping out in the AADvac1 arm and 20.3% in the placebo arm. The per-protocol (PP) set comprised patients who completed the study and had no important protocol deviations ($n=162$). The per-protocol responder set (PPR) consisted of AADvac1-treated patients who developed an IgG antibody response to the Axon Peptide 108 component of AADvac1 and all placebo-treated study completers ($n=160$; Fig. 1). The results of the PP and PPR sets are supportive of the main analysis of the FAS set (Supplementary Table 27).

There were no statistically significant differences in any of the demographic characteristics in the FAS at baseline (Table 1).

The baseline characteristics of patients with longitudinal CSF and DTI data and of subgroups are in the Supplementary Section 6.

It is important to note that patients could fulfill the biomarker inclusion criterion (no. 4) either via positivity for CSF tau and amyloid biomarkers or by displaying medial temporal lobe atrophy in MRI. As a result, a proportion of patients who were negative for CSF biomarkers was enrolled solely based on medial temporal lobe atrophy in MRI. Of 46 patients with available baseline CSF samples, 4% displayed values outside the AD cutoff for CSF $A\beta_{1-42}$, 28% for total tau and 33% for pT181 tau. Universally, patients whose pT181 levels were below the cutoff displayed similarly low values for total tau and borderline values for $A\beta_{1-42}$ (Extended Data Fig. 1).

Primary end-point results for AADvac1 safety. Treatment-emergent serious adverse events (SAEs) were seen in 17.1% of individuals treated with AADvac1 (29 events in $n=20$ individuals) and in 24.1% of placebo-treated individuals (32 events in $n=19$ individuals) (safety set, relative risk of 0.711, 95% CI (0.410, 1.240), two-sample Wald z-statistic of 1.197; risk difference, −7.04% upper bound of 90% CI 0.556%) (Supplementary Table 18).

Reversible injection-site reactions (ISRs) were the only adverse event (AE) occurring with pronouncedly higher frequency in AADvac1-treated individuals; ISRs were reported in 47.0% of AADvac1-treated individuals and in 25.3% of placebo-treated individuals (AADvac1 $n=55$, placebo $n=20$, two-sample Wald z-statistic of 2.855, $P=0.004$, relative risk of 1.857, 95% CI (1.214, 2.840); risk difference of 21.13, upper bound of 90% CI 29.7%) (Supplementary Table 16). A statistically significant difference was observed in the incidence of confusion, in 5.1% AADvac1-treated individuals and in no placebo-treated individuals (AADvac1 $n=6$, placebo $n=0$, two-sample Wald z-statistic of 2.044, $P=0.041$, relative risk 95% CI (1.086, infinity) (as the incidence in one arm was 0, relative risk could not be calculated and the CI was calculated using Koopman's asymptotic score method[28]; risk difference of 46.5%, upper bound of 90% CI 7.83%). The confusion was transient and self-limiting in five of six cases. Otherwise, the observed AEs and SAEs were in line with the background incidence expected in the elderly AD population; no safety signal emerged. A logistic regression analysis of AE incidence for each system organ class (SOC) where ≥5% of study participants experienced an AE (with treatment group, age, sex and pooled country as covariates) did not reveal any additional safety findings (for each system organ class (SOC), the odds ratios of AADvac1 to placebo are not statistically significantly different from one at a significance level of 0.05; Table 2). All treatment-emergent SAEs designated as suspected unexpected serious adverse reactions by the investigators occurred in placebo-treated individuals.

Two individuals on active treatment died; however, their deaths were considered to be unrelated to treatment by the Data and Safety

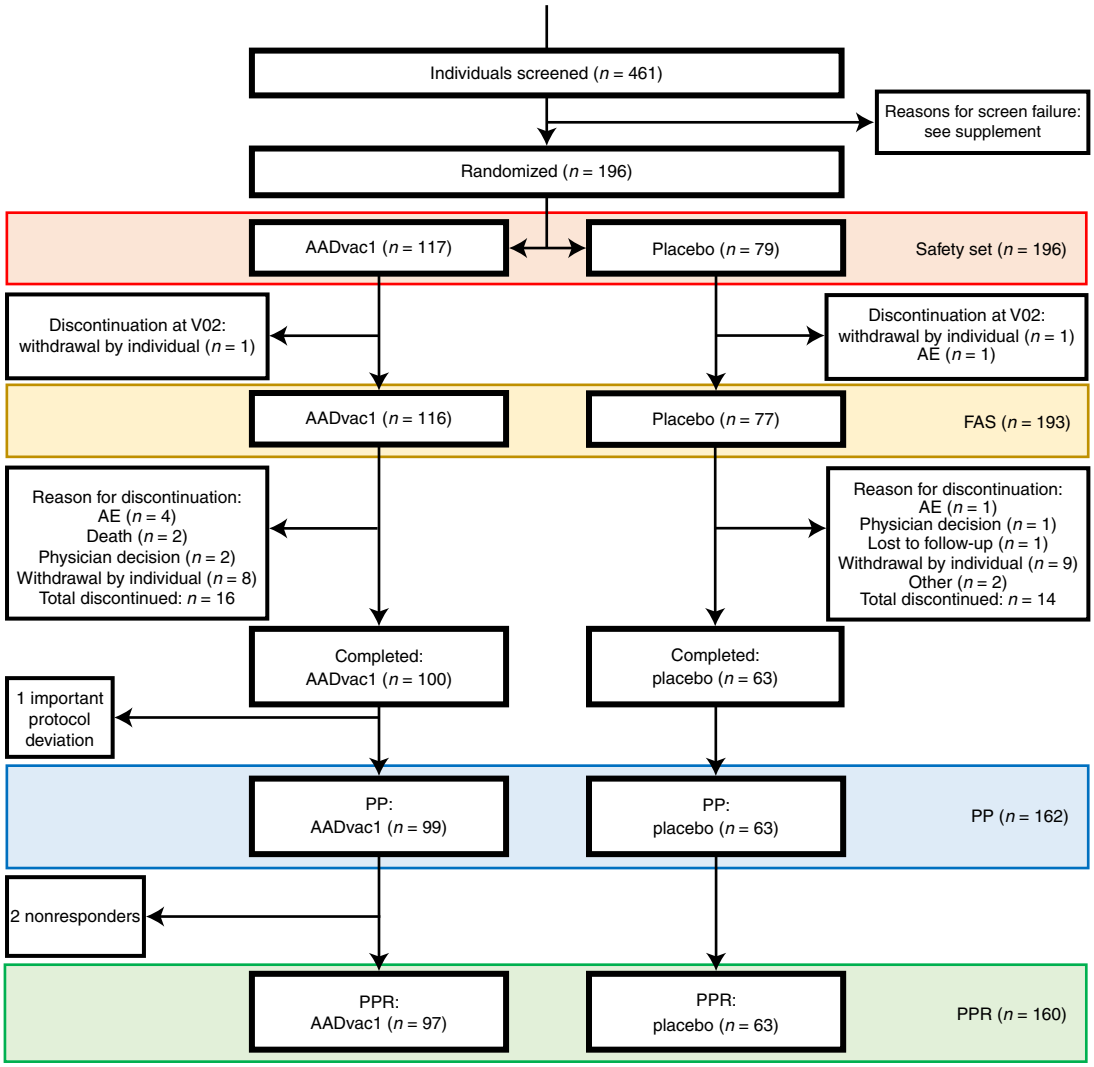

Fig. 1 | Individual disposition flowchart. Flowchart showing individual disposition.

Monitoring Board (DSMB) and investigators. One individual experienced emesis during an examination and aspirated vomit, resulting in respiratory failure. The other individual had pre-existing cardiac risk factors (ischemic heart disease; status post-stenting of coronary arteries; body mass index of 32; first degree atrioventricular block) and experienced cardiac arrest.

No statistically significant differences in laboratory safety parameters (hematology, coagulation, chemistry and urinalysis) and vital signs were observed.

No vascular edema was observed in MRI. There was no statistically significant difference in incidence of micro-hemorrhages (MHs). Newly occurring MH were observed in 17.54% of AADvac1-treated individuals and in 9.33% of placebo-treated individuals (AADvac1 $n=20$, $N=114$, placebo $n=7$, $N=75$, two-sample z-statistic of 1.527, $P=0.127$, relative risk of 1.880, 95% CI (0.836, 4.225); risk difference of 7.714%, upper bound of 90% CI 14.105%). Newly occurring superficial cortical siderosis was observed in two patients on AADvac1 treatment and three patients on placebo.

Incidence of AEs by SOC and a full listing of SAEs are presented in Supplementary Table 17. Incidence of AEs observed in ≥5% of trial participants is presented in Table 2.

The independent DSMB concluded in its final report that no significant safety concerns that would prevent the continued development of AADvac1 were identified in the ADAMANT trial.

Secondary end-point results for AADvac1 immunogenicity. AADvac1 was highly immunogenic, with patients reaching a geometric mean IgG titer of 1:17,350 (95% CI (12,809, 23,500)) against Axon Peptide 108 (the tau epitope in AADvac1) after the initial six doses (week 24, $n=114$). Boosters were effective at maintaining this response. In the intervals between booster vaccinations (14 weeks after the sixth dose or previous booster), geometric mean titers declined to a mean of 52% of the response measured 4 weeks after the sixth dose or last booster and were restored to previous levels by booster doses. Responder rate (percentage of patients with IgG titer more than lower limit of quantitation) was 96.5% at the end of the initial six-dose regimen and 98.3% overall (Fig. 2a). The titers corresponded quantitatively to a geometric mean response of 1.959 μg ml^{-1} of induced IgG (95% CI (1.596, 2.405)) after six doses (Fig. 2b), as measured by quantitative ELISA. Younger patients displayed a tendency to produce higher antibody titers (Pearson r −0.2335 (95% CI −0.4119, −0.03785), $P=0.0200$; Spearman $r=-0.1407$, 95% CI (−0.3343, 0.06420)) (Extended Data Fig. 2).

Antibody levels in the serum and CSF correlate closely (Extended Data Fig. 3). The IgG subclass assessment was performed cross-sectionally after 4–5 doses. The response in tested patients ($n=13$) was IgG1-dominated, with 12 of 13 patients producing mostly or exclusively antibodies of the IgG1 isotype. The IgG response consisted of 64.97% (54.41, 77.57) IgG1, 0.22% (0.05, 0.91) IgG2,

Table 1 | Baseline demographics (FAS)

	AADvac1 ($n=116$)	Placebo ($n=77$)	Total ($n=193$)
Age (years) (mean, s.d.)	70.5 (8.33)	72.7 (6.86)	71.4 (7.83)
Time since AD diagnosis (months) (mean, s.d.)	24.4 (25.57)	24.6 (16.90)	24.5 (22.47)
Sex (% male/female)	47.4/52.6	41.6/58.4	45.1/54.9
Ethnic origin (%)	White: 100.0	White: 100.0	White: 100.0
Education (years) (mean, s.d.)	12.9 (3.49)	12.2 (3.33)	12.6 (3.44)
Concomitant AChEI treatment (*n*, %)	116 (100.0)	77 (100.0)	193 (100.0)
Concomitant memantine treatment (*n*, %)	17 (14.7)	12 (15.6)	29 (15.0)
MMSE (mean, s.d.)	23.0 (1.90)	23.2 (1.95)	23.1 (1.91)
CDR-SB (mean, s.d.)	4.4 (2.08)	4.5 (2.43)	4.4 (2.22)
***APOE4* (*n*, %)**	Noncarrier: 47 (40.5%) Heterozygote: 56 (48.3%) Homozygote: 13 (11.2%)	Noncarrier: 26 (33.8%) Heterozygote: 39 (50.6%) Homozygote: 12 (15.6%)	Noncarrier: 73 (37.8%) Heterozygote: 95 (49.2%) Homozygote: 25 (13.0%)
Hippocampal atrophy score (*n*, %)	Scheltens 0: 0 (0%) Scheltens 1: 3 (2.6%) Scheltens 2: 68 (58.6%) Scheltens 3: 36 (31.0%) Scheltens 4: 9 (7.8%)	Scheltens 0: 0 (0%) Scheltens 1: 0 (0%) Scheltens 2: 49 (63.6%) Scheltens 3: 21 (27.3%) Scheltens 4: 7 (9.1%)	Scheltens 0: 0 (0%) Scheltens 1: 3 (1.6%) Scheltens 2: 117 (60.6%) Scheltens 3: 57 (29.5%) Scheltens 4: 16 (8.3%)
White matter lesion score (*n*, %)	Fazekas 0: 16 (13.8%) Fazekas 1: 71 (61.2%) Fazekas 2: 29 (25.0%) Fazekas 3: 0 (0%)	Fazekas 0: 12 (15.6%) Fazekas 1: 49 (63.6%) Fazekas 2: 16 (20.8%) Fazekas 3: 0 (0%)	Fazekas 0: 28 (14.5%) Fazekas 1: 120 (62.2%) Fazekas 2: 45 (23.3%) Fazekas 3: 0 (0%)
NfL in plasma (pg ml^{-1}, mean and 95% CI)	21.08 (19.47,22.68)	20.56 (19.05,22.08)	20.76 (19.67,21.86)

AChEI, acetylcholinesterase inhibitor; MMSE, mini mental state examination; NfL, neurofilament light chain protein.

18.80% (7.24, 48.86) IgG3 and 0.04% (0.03, 0.06) IgG4 (geometric mean, 95% CI) (Extended Data Fig. 4).

Secondary end-point results for clinical outcomes. Placebo-verum differences in clinical outcome measures were evaluated in the FAS (AADvac1 $n=100$, placebo $n=63$ at week 104) by a predefined analysis of covariance (ANCOVA) model with stepwise selection (Table 3) with treatment group, pooled country, sex, age, years of education, *APOE4* status, baseline MRI hippocampal volume, baseline Clinical Dementia Rating-Sum of the Boxes (CDR-SB) scale and baseline of the given assessment as covariates.

None of the comparisons was statistically significant at the level of $P=0.05$. In summary, neither positive nor negative effects of AADvac1 treatment on cognition and function were detectable in this sample.

Exploratory analyses on fluid biomarker and neuroimaging measurements. Plasma levels of neurofilament light-chain protein (NfL), an emerging biomarker of ongoing neurodegeneration and a promising prognostic marker of AD dementia[29], were balanced between the groups at baseline (Fig. 3a). On the FAS completers, AADvac1 treatment induced separation between the AADvac1-treated and the placebo arm. The mean change from baseline (95% CI) in the AADvac1 group was 2.10 (0.99, 3.19) pg ml^{-1} ($n=100$), corresponding to a 12.6% increase over 104 weeks; in the placebo group, the change was 4.93 (3.31, 6.55) pg ml^{-1} ($n=63$), a 27.7% increase over 104 weeks (two-sample t-statistic $=-2.893$, d.f. $=117.66$, $P=0.0046$, mean difference $=-2.84$, 95% CI (-4.78, -0.89). The mean difference adjusted for baseline NfL levels $=-2.79$, 95% CI (-4.65, -0.93) pg ml^{-1}, t-statistic $=-2.9639$, d.f. $=160$, $P=0.0035$. This difference translates to a standardized effect size of Cohen's $d=-0.481$ (-0.804, -0.164) and a relative attenuation in NfL increase over time of 58% in comparison to placebo (Fig. 3b).

We explored the possible effect of AADvac1 on the levels of CSF tau biomarkers in all patients who provided both baseline and end-of-study samples ($n=27$, AADvac1 $n=20$, placebo $n=7$). Reductions in all investigated CSF tau markers were observed in the AADvac1-treated group in comparison to placebo, with moderate to large effect sizes; after baseline adjustments a statistically significant reduction was observed for tau species phosphorylated on Thr217 and trends $P<0.1$ on tau species phosphorylated on Thr181 and total tau. All analyses list the ANCOVA P value, with treatment and baseline values for the respective biomarkers used as covariates (Table 4 and Extended Data Fig. 5). Change in CSF tau biomarkers by *APOE* genotype is shown in Extended Data Fig. 6.

The impact of AADvac1 treatment on amyloid-β_{1-40} and neurogranin in the CSF was minor and no difference was observed on amyloid-β_{1-42} (Extended Data Fig. 7).

In FAS completers, no meaningful difference in brain atrophy rates between AADvac1-treated and placebo-treated group was observed in volumetric analyses ($n=163$; 7 MRIs were not evaluable due to movement artifacts). The following regions of interest were pre-specified as exploratory end points and percentage volume change from baseline at week 104 evaluated via mixed model with repeated measures (MMRM) analysis (AADvac1 $n=95$, placebo $n=61$): whole brain (least squares (LS) mean (s.e.m.) 0 (0.313), 95% CI (-0.62, 0.61), $P=0.991$); left hippocampus (LS mean (s.e.m.) -0.28 (0.711), 95% CI (-1.68, 1.12), $P=0.696$); right hippocampus (LS mean (s.e.m.) -0.71 (0.694), 95% CI (-2.08, 0.66), $P=0.310$); left entorhinal cortex (LS mean (s.e.m.) 0.22 (1.289), 95% CI (-2.32, 2.77), $P=0.862$); and right entorhinal cortex (LS mean (s.e.m.) 0.07 (1.395), 95% CI (-2.68, 2.82), $P=0.960$. Similarly, no significant difference was observed on regions of interest evaluated as research objectives (whole cortex, lateral ventricles, frontal cortex, temporal cortex, occipital cortex, parietal cortex and basal ganglia).

Table 2 | Adverse events by SOC, observed in ≥5% of the trial participants

SOC	AADvac1	Placebo	Total		
Preferred term	**(*N* = 117)**	**(*N* = 79)**	**(*N* = 196)**	**Logistic regression odds ratio (*P* value)**	**Risk difference in % (upper bound of 90% CI)**
	***n* (%) [E]**	***n* (%) [E]**	***n* (%) [E]**		
All TEAEs	99 (84.6) [827]	64 (81.0) [503]	163 (83.2) [1,330]	1.30 (0.517)	3.79 (10.904)
Infections and infestations	**52 (44.4) [125]**	**44 (55.7) [77]**	**96 (49.0) [202]**	**0.60 (0.092)**	**−11.02 (−1.844)**
Nasopharyngitis	19 (16.2) [34]	12 (15.2) [15]	31 (15.8) [49]		
Urinary tract infection	14 (12.0) [21]	12 (15.2) [22]	26 (13.3) [43]		
Upper respiratory tract infection	9 (7.7) [14]	7 (8.9) [9]	16 (8.2) [23]		
Investigations	**41 (35.0) [106]**	**29 (36.7) [65]**	**70 (35.7) [171]**	**0.92 (0.796)**	**−1.74 (7.134)**
N-terminal prohormone brain natriuretic peptide increased	11 (9.4) [12]	4 (5.1) [4]	15 (7.7) [16]		
Blood folate decreased	7 (6.0) [7]	7 (8.9) [7]	14 (7.1) [14]		
Fibrin D dimer increased	7 (6.0) [8]	10 (12.7) [12]	17 (8.7) [20]		
Nervous system disorders	**41 (35.0) [125]**	**28 (35.4) [60]**	**69 (35.2) [185]**	**0.93 (0.821)**	**−0.51 (8.330)**
Headache	22 (18.8) [55]	13 (16.5) [23]	35 (17.9) [78]		
Dizziness	12 (10.3) [17]	9 (11.4) [10]	21 (10.7) [27]		
Gastrointestinal disorders	**36 (30.8) [80]**	**22 (27.8) [56]**	**58 (29.6) [136]**	**1.08 (0.821)**	**2.70 (11.111)**
Vomiting	9 (7.7) [14]	2 (2.5) [5]	11 (5.6) [19]		
Diarrhea	8 (6.8) [10]	10 (12.7) [14]	18 (9.2) [24]		
Nausea	7 (6.0) [18]	5 (6.3) [9]	12 (6.1) [27]		
Psychiatric disorders	**33 (28.2) [67]**	**16 (20.3) [30]**	**49 (25.0) [97]**	**1.41 (0.331)**	**7.58 (15.444)**
Depression	7 (6.0) [7]	3 (3.8) [3]	10 (5.1) [10]		
Confusional state	6 (5.1) [7]	0	6 (3.1) [7] *		
Musculoskeletal and connective tissue disorders	**30 (25.6) [45]**	**18 (22.8) [35]**	**48 (24.5) [80]**	**1.18 (0.639)**	**2.59 (10.530)**
Arthralgia	7 (6.0) [7]	3 (3.8) [5]	10 (5.1) [12]		
Back pain	7 (6.0) [8]	5 (6.3) [8]	12 (6.1) [16]		
Injury, poisoning and procedural complications	**25 (21.4) [45]**	**13 (16.5) [17]**	**38 (19.4) [62]**	**1.40 (0.379)**	**4.57 (11.814)**
Contusion	7 (6.0) [9]	3 (3.8) [3]	10 (5.1) [12]		
General disorders and administration site conditions	**24 (20.5) [44]**	**14 (17.7) [28]**	**38 (19.4) [72]**	**1.14 (0.733)**	**2.49 (9.804)**
Fatigue	13 (11.1) [25]	6 (7.6) [13]	19 (9.7) [38]		
Skin and subcutaneous tissue disorders	**18 (15.4) [30]**	**7 (8.9) [9]**	**25 (12.8) [39]**	**1.88 (0.189)**	**6.09 (12.137)**
Renal and urinary disorders	**17 (14.5) [29]**	**10 (12.7) [15]**	**27 (13.8) [44]**	**1.15 (0.741)**	**1.55 (7.989)**
Cardiac disorders	**16 (13.7) [23]**	**14 (17.7) [29]**	**30 (15.3) [52]**	**0.80 (0.586)**	**−4.23 (2.659)**
Metabolism and nutrition disorders	**15 (12.8) [19]**	**7 (8.9) [9]**	**22 (11.2) [28]**	**1.52 (0.390)**	**3.57 (9.409)**
Vascular disorders	**15 (12.8) [25]**	**15 (19.0) [24]**	**30 (15.3) [49]**	**0.65 (0.282)**	**−6.31 (0.635)**
Hypertension	11 (9.4) [15]	6 (7.6) [8]	17 (8.7) [23]		
Respiratory, thoracic and mediastinal disorders	**14 (12.0) [21]**	**12 (15.2) [15]**	**26 (13.3) [36]**	**0.78 (0.569)**	**−3.44 (3.077)**
Eye disorders	**10 (8.5) [17]**	**7 (8.9) [10]**	**17 (8.7) [27]**	**0.92 (0.881)**	**−0.63 (4.810)**
Ear and labyrinth disorders	**6 (5.1) [6]**	**3 (3.8) [5]**	**9 (4.6) [11]**		
Neoplasms benign, malignant and unspecified (incl. cysts and polyps)	**6 (5.1) [9]**	**2 (2.5) [3]**	**8 (4.1) [12]**		
Blood and lymphatic system disorders	**5 (4.3) [5]**	**6 (7.6) [6]**	**11 (5.6) [11]**		
Hepatobiliary disorders	**3 (2.6) [3]**	**2 (2.5) [2]**	**5 (2.6) [5]**		
Reproductive system and breast disorders	**3 (2.6) [3]**	**4 (5.1) [4]**	**7 (3.6) [7]**		

Continued

Table 2 | Adverse events by SOC, observed in ≥5% of the trial participants (Continued)

SOC	AADvac1	Placebo	Total		
Preferred term	**(*N* = 117)**	**(*N* = 79)**	**(*N* = 196)**	**Logistic regression odds ratio (*P* value)**	**Risk difference in % (upper bound of 90% CI)**
	***n* (%) [E]**	***n* (%) [E]**	***n* (%) [E]**		
Immune system disorders	0	2 (2.5) [2]	2 (1.0) [2]		
Product issues	0	1 (1.3) [1]	1 (0.5) [1]		
Surgical and medical procedures	0	1 (1.3) [1]	1 (0.5) [1]		

AEs were coded using MedDRA, v.21.1. Events that were classified as ISRs are not included in this table. AEs are shown by incidence in the AADvac1 arm in descending order, if seen in ≥5% of trial participants ($n \geq 10$) or if a significant difference in incidence was observed, regardless of allocation. For SOC with no AEs ≥ 5%, only the overall incidence is shown; for SOC with overall incidence of AEs < 5%, no formal statistical comparison is made. *Incidence significantly different at $P < 0.05$. Logistic regression (with age, sex and pooled country as covariates) two-sample Wald test *P* values are listed for all SOC where ≥5% of patients experienced an AE, null hypotheses about adjusted odds ratio are tested against two-sided alternatives, *P* values are not corrected for multiplicity. Empirical one-sided Wald 90% CI for risk difference (with upper bound) is also shown. TEAE, treatment-emergent adverse event; [E], total number of occurrences of the given AE.

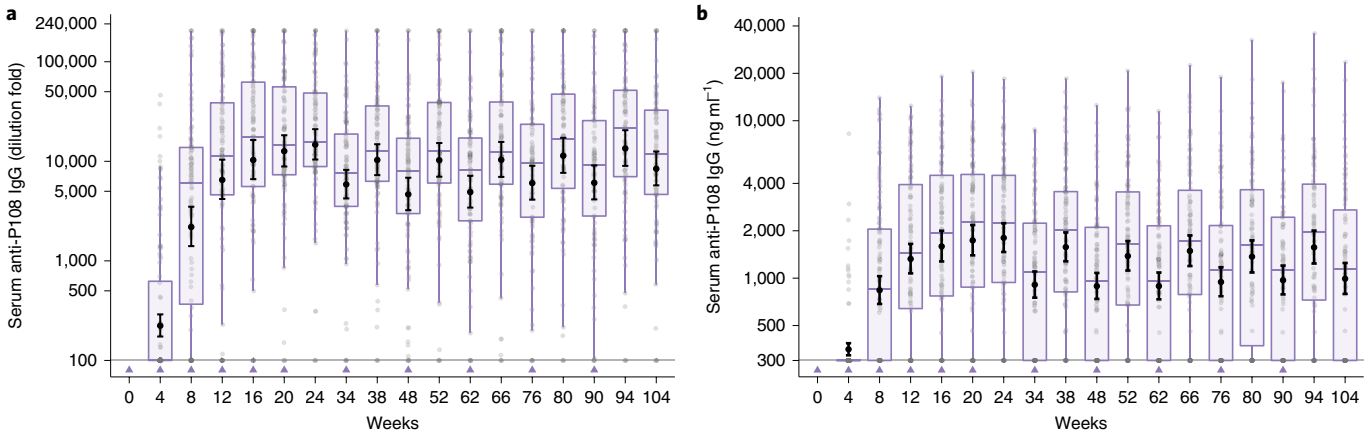

Fig. 2 | Antibody response over 104 weeks of AADvac1 treatment indicates robust immunogenicity. a, AADvac1 treatment induces progressively higher antibody titers with each of the initial six doses. Achieved antibody levels are maintained by boosters at 3-month intervals. AADvac1 was administered at weeks 0, 4, 8, 12, 16, 20, 34, 48, 62, 76 and 90 (violet triangles on *x* axis). **b**, Antibody levels as measured by quantitative ELISA display the same pattern as the titer measurement. Descriptive statistics and sample sizes for each visit are shown in Supplementary Tables 19 and 20. Thick vertical lines and error bars indicate geometric mean and 95% CI. Boxes indicate median and quartiles. Whiskers indicate 1.5× interquartile range (IQR). Values in the AADvac1 group are shown (FAS, $n = 116$ at week 4, $n = 114$ at week 24, $n = 99$ at week 104; one sample each at weeks 94 and 104 was not evaluable); no quantifiable response to Axon Peptide 108 was observed in the placebo arm.

Fractional anisotropy (FA) and mean diffusivity (MD) were evaluated using diffusion tensor imaging as measures of white matter organization and integrity; baseline and end-of-study diffusion tensor imaging (DTI) sequences were not an obligatory part of the MRI protocol and were recorded in 20 patients of the FAS (AADvac1 $n = 13$, placebo $n = 7$). A reduction of FA and an increase in MD occurs during the neurodegenerative process as tissue organization deteriorates and barriers to diffusion decay. Compared to placebo, treatment with AADvac1 stabilized FA and MD in the fornix, a white matter tract that is highly relevant in AD as it originates from the hippocampus. Similar stabilization of FA and MD, although not statistically significant, was seen in the corpus callosum, with a fronto-dorsal gradient (Table 4 and Extended Data Fig. 8; change in DTI measures by *APOE* genotype is shown in Extended Data Fig. 9).

Post hoc analyses on a subgroup of patients predicted to have both amyloid and tau pathology

AD core CSF biomarker analysis of the patients' CSF samples available at baseline ($n = 46$) showed that 33% did not fulfill AD diagnostic criteria (total tau protein > 400 pg ml^{-1}, p-tau T181 protein > 60 pg ml^{-1}, Aβ42 < 600 pg ml^{-1}), with 13 patients failing only pT181 cutoff and 2 patients failing both amyloid-β and pT181 cutoffs. This indicated that out of the majority of patients recruited solely on MRI criteria (Scheltens score) a sizable portion might not fulfill AD CSF biomarker cutoffs.

As the study population contained a mixture of patients who were positive or negative for the AD biomarker, a multimodal classifier combining structural MRI, demography and clinical modalities[30–32] was utilized to identify a subset of patients most likely to be positive for amyloid and tau pathology. In this subgroup post hoc analysis (AADvac1 $n = 62$ (54 completers), placebo $n = 47$ (39 completers)), a slower clinical and functional decline as measured by the CDR-SB and Alzheimer's Disease Cooperative Study (ADCS)-mild cognitive impairment (MCI)-Activities of Daily Living (ADL) scales was observed. The effect on NfL was also replicated in this subgroup; MRI volumetry analyses were inconclusive (Table 5).

Discussion

The ADAMANT study was designed to evaluate the safety and tolerability (primary objective), immunogenicity and clinical efficacy (secondary objectives) and fluid and imaging biomarkers (exploratory and research objectives) of the active tau vaccine AADvac1 in patients with mild AD.

The study shows that AADvac1 treatment was well tolerated over the 104-week study period. This finding was independently confirmed by a DSMB that monitored the safety of the vaccine for

Table 3 | Clinical outcomes and biomarker outcomes (FAS)

FAS group (clinical outcomes, secondary end points)								
Change from baseline (104w)	**AADvac1 (*n*)**	**placebo (*n*)**	**AADvac1 (mean change)**	**Placebo (mean change)**	**Adjusted mean difference[a]**	**95% CI[a]**	***P* value[a]**	**Cohen's *d***
CDR-SB	97	61	3.077	3.164	−0.3600	(−1.306, 0.589)	0.456	−0.028
CCB8 score	90	56	−0.303	−0.231	0.0008	(−0.169, 0.172)	0.993	−0.138
ADCS-MCI-ADL 24	96	61	−11.104	−9.639	1.1000	(−1.760, 3.900)	0.457	−0.124

[a]ANCOVA, adjusted as per Supplementary Section 9. For all analyses, the completers in the FAS (AADvac1 $n=100$, placebo $n=63$) who possess a baseline and end-of-study value for the given assessment were used. Due to progression of dementia, some patients were not able to complete the cognitive battery and/or CDR-SB; ADL assessment is missing in some patients due to unavailability of the caregiver. Two-sided Wald 95% CI of adjusted mean difference, null hypotheses about adjusted mean difference are tested against two-sided alternatives, *P* values are not corrected for multiplicity.

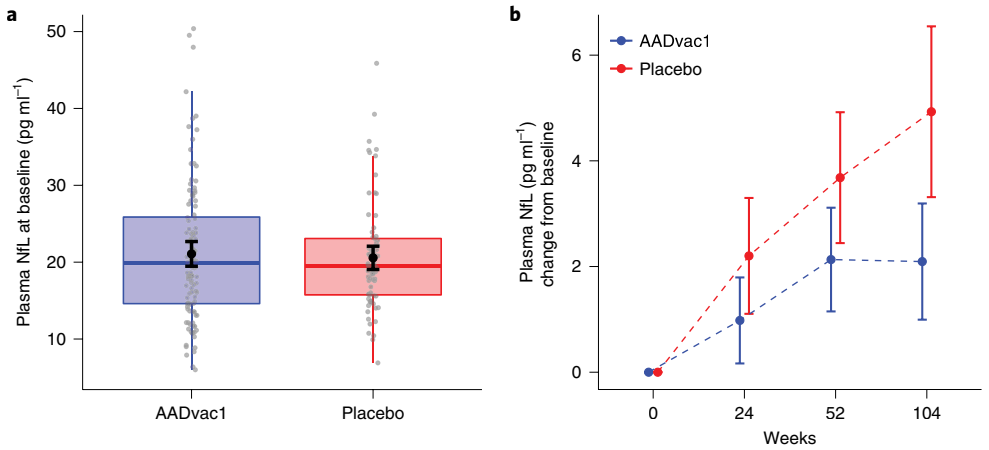

Fig. 3 | AADvac1 treatment significantly slowed the increase in levels of plasma NfL. a, Neurofilament light-chain levels in plasma are balanced between study arms at baseline. The *y* axis is truncated at 50 pg ml^{-1}. Filled circles and thick vertical lines indicate mean and 95% CI. Boxes indicate median and quartiles. Whiskers indicate 1.5 × IQR. Three outliers (one in the AADvac1 group (65.9 pg ml^{-1}) and two in the placebo group (64.4 and 134.8 pg ml^{-1})) are not shown. **b**, AADvac1-treatment mitigates the neurofilament light-chain protein (NfL) increase over time, suggesting a slowing of neurodegeneration. Change from baseline (mean, two-sided Wald 95% CI of mean) are shown; AADvac1, $n=100$; placebo, $n=63$ (FAS, completers); ANCOVA adjusted for baseline NfL, 95% CI −4.6469, −0.9305; *t*-statistic = −2.9639; d.f. = 160; $P=0.0035$; Cohen's $d=-0.4811$.

the duration of study. Notably, no clinically significant adverse findings were attributable to AADvac1 with respect to laboratory tests or physical assessment. Confusion (transient in all but one case) was observed in six AADvac1-treated patients. As confusion naturally occurs in patients with AD, a larger study is required to evaluate whether this is an adverse reaction or a chance observation; currently it constitutes a potential risk of moderate importance. The only AEs clearly associated with AADvac1 treatment were ISRs, which are to be expected with subcutaneous injection of an immunogen with aluminum hydroxide adjuvant. Patients treated with placebo (adjuvant in buffer) also displayed these reactions, albeit at a lower frequency; thus, placebo was efficient at masking treatment allocation. The excellent safety profile of AADvac1 makes it suitable for longer studies of prevention in at-risk individuals with biomarker evidence of the AD pathophysiological process. Asymptomatic carriers of dominant AD mutations in the amyloid pathway (APP, PSEN1 or PSEN2) could also benefit from preventive AADvac1 treatment, as the onset and progression of clinical symptoms in these patients align with propagation of tau pathology[33,34].

The secondary end points (CDR-SB, custom cognitive battery (CCB) assessing multiple domains of cognition and ADCS-MCI-ADL) did not show significant benefit to treated patients in the entire study sample. With 193 patients in the FAS, the study was powered to detect only large effects on clinical end points. Furthermore, of 46 patients who consented to the collection of CSF, 33% did not fulfill criteria for AD diagnostic biomarkers, predominantly failing to meet total tau and phospho-tau cutoffs. This analysis showed that the therapeutic target, tau protein pathology, was not present in all ADAMANT patients. In a post hoc attempt to analyze the effect of AADvac1 treatment on patients with AD pathophysiology, we took advantage of a multimodal classifier prediction model developed recently (based on the algorithm presented elsewhere[35]) and identified 109 patients (93 completers) who were most likely to be positive for both amyloid and tau biomarkers. In this amyloid- and tau-positive group, we observed an effect on CDR-SB and ADCS-MCI-ADL, as well as plasma NfL, which suggests that treatment may slow down cognitive and functional decline in patients with AD having both amyloid and tau pathology and perhaps, fewer comorbidities. We recognize that these post hoc analyses come with important limitations as they were not pre-specified in the clinical study protocol and were not corrected for multiplicity testing. These results must therefore be interpreted with caution and will require confirmation in future clinical development.

AADvac1 elicited production of high levels of antibodies in the elderly AD population with an overall responder rate of 98.3% over the course of study. The almost universal seroconversion is in contrast with numerous studies reporting high failure rates of vaccination against influenza, pneumococcal pneumonia and herpes zoster in the elderly[36]. The overall impact of patient age on AADvac1-induced IgG response was minor, although the best responders were found in the younger segment of the study population. Sera from our phase 1 study patients showed that the

Table 4 | Fluid biomarker assessments and neuroimaging measurements

FAS group (biomarker outcomes, exploratory and research end points)								
Change from baseline (104w)	**AADvac1 (*n*)**	**placebo (*n*)**	**AADvac1 (mean change)**	**Placebo (mean change)**	**Adjusted mean difference[a]**	**95% CI[a]**	***P* value[a]**	**Cohen's *d***
Plasma NfL (pg ml^{-1})	100	63	2.094	4.929	−2.789	(−4.647, −0.931)	0.00350	−0.4811
Total cortex volume (%)	93	61	−3.147	−3.056	−0.089	(−1.354, 1.176)	0.88981	−0.0235
Temporal cortex volume (%)	93	61	−5.755	−5.843	0.122	(−1.407, 1.651)	0.87488	0.0185
Total hippocampal volume (%)	93	61	−8.726	−8.068	−0.863	(−2.271, 0.546)	0.22827	−0.1508
Lateral ventricles volume (%)	93	58	18.877	17.994	1.038	(−2.518, 4.595)	0.56481	0.0813
FA fornix	13	7	0.030	−0.048	0.079	(0.029, 0.128)	0.00361	1.9261
MD fornix (10^{-3} mm^2 s^{-1})	13	7	−0.194	0.191	−0.298	(−0.637, 0.041)	0.08135	−1.3254
FA genu CC	13	7	0.003	−0.028	0.023	(−0.008, 0.055)	0.13324	0.9732
MD genu CC (10^{-3} mm^2 s^{-1})	13	7	0.015	0.073	−0.053	(−0.11, 0.005)	0.07097	−1.0913
CSF p-tau T181 (pg ml^{-1})	20	7	−6.288	0.286	−8.126	(−17.908, 1.657)	0.09935	−0.5749
CSF p-tau T217 (pg ml^{-1})	19	7	−34.448	30.164	−69.253	(−119.182, −19.323)	0.00867	−0.9474
CSF t-tau (pg ml^{-1})	20	7	−9.931	63.786	−71.836	(−148.189, 4.516)	0.06399	−0.8963

[a]ANCOVA, adjusted for baseline value of the given assessment. For all analyses, completers in the FAS (AADvac1 $n=100$, placebo $n=63$) who possess a baseline and end-of-study value for the given assessment were used. In some patients, movement artifacts precluded the evaluation of volumetry. A total of 20 patients provided baseline and end-of study DTI sequences; a total of 27 patients provided both baseline and end-of-study CSF samples. In one patient, the pT217 marker could not be evaluated because samples were depleted. Two-sided Wald 95% CI of adjusted mean difference, null hypotheses about adjusted mean difference are tested against two-sided alternatives, *P* values are not corrected for multiplicity. Four statistical comparisons were made for DTI, 6 for CSF biomarkers and 12 for MRI volumetry. CC, corpus callosum.

Table 5 | Post hoc analyses on an algorithm-defined amyloid- and tau-positive subgroup of patients with AD

Algorithm-defined amyloid- and tau-positive subgroup								
Change from baseline (104w)	**AADvac1 (*n*)**	**placebo (*n*)**	**AADvac1 (mean change)**	**Placebo (mean change)**	**Adjusted mean difference[a]**	**95% CI[a]**	***P* value[a]**	**Cohen's *d***
CDR-SB	53	38	3.24	4.08	−1.17	(−2.32, −0.01)	0.04809	−0.273
MMSE score	53	37	−5.68	−6.38	1.35	(−0.78, 3.48)	0.21000	0.129
ADCS-MCI-ADL 24	52	37	−10.92	−13.24	4.25	(0.23, 8.28)	0.03874	0.216
Plasma NfL (pg ml^{-1})	54	39	1.91	5.51	−3.35	(−5.91, −0.79)	0.01078	−0.585
Total cortex volume (%)	51	37	−3.459	−3.940	0.830	(−0.777, 2.436)	0.30741	0.120
Temporal cortex volume (%)	51	37	−6.207	−7.038	1.023	(−0.881, 2.926)	0.28828	0.176
Total hippocampal volume (%)	51	37	−9.448	−8.931	−0.488	(−2.324, 1.348)	0.59836	−0.122
Lateral ventricles volume (%)	51	34	19.238	20.919	−1.563	(−5.251, 2.124)	0.40134	−0.162

[a]ANCOVA, adjusted for baseline value of the given assessment, age and baseline plasma NfL. Two-sided Wald 95% CI of adjusted mean difference, null hypotheses about adjusted mean difference are tested against two-sided alternatives. *P* values are reported without correction for multiplicity and the number of comparisons was 4 for clinical assessments and 12 for MRI volumetry assessments.

affinity of AADvac1-induced antibodies was pronouncedly higher for pathological tau than for physiological tau[26,27]. Upon binding, these antibodies are expected to inhibit tau aggregation by interfering with the assembly process of AD tau filaments[22] and protect healthy neurons from the entry of seeding-capable 'tauons' and thus from propagation of tau pathology[23]. This is in line with several preclinical studies on passive tau immunotherapy, where anti-tau antibodies efficiently blocked tau spreading and thus reduced tau pathology in animal models[37,38]. Our recent study showed that serum antibodies label pathological tau for removal by microglia via an $F_C\gamma$II–III receptor-dependent mechanism[24]. The antibodies thus intercept the crucial extracellular step of tau pathology propagation and via binding and reducing the levels of seeding-capable tau should result in deceleration of the neurodegenerative process[17]. Our current data are in line with previous findings from phase 1 and indicate that AADvac1-induced antibodies are mainly IgG1 and IgG3 isotypes, which both strongly engage Fc receptors[27]. In contrast, the Fc fragment of the antibody is probably not involved in the mechanism of action of several humanized IgG4 anti-tau antibodies, such as ABBV 8E12, RO7105705, UCB0107 or BIIB092. Consequently, those compounds may have limited ability to internalize extracellular tau via Fc receptors[16].

Tau and p-tau in CSF are established biomarkers of neurodegeneration and tau pathology, respectively[39] and are used to assess target engagement of tau-targeted drugs[40]. A statistically significant effect was observed on pT217 tau; nonstatistically different trends ($P<0.1$) were observed on total tau and pT181 tau after baseline levels of the respective biomarker were used as covariates in the analysis. We and others have shown that CSF p-tau pT217 outperforms p-tau pT181 as a biomarker for AD. CSF p-tau217 also

better mirrors tau pathology measured by PET imaging at different AD stages[41–44]. The fact that the AADvac1 − placebo difference on p-tau pT217 becomes more pronounced when baseline levels of pT217 are taken into account further supports the hypothesis that tau-targeting therapies are best employed in patients whose neurodegeneration is primary driven by tau pathology (those with high p-tau levels), as opposed to patients with extensive non-AD pathology (such as limbic-predominant age-related TDP-43 encephalopathy[45]). In line with this, generally a more pronounced reduction in pT217 was seen in AADvac1-treated patients with higher baseline levels, whereas in patients with low baseline pT217, the levels of the marker remained rather stable. Out of caution, we recognize that these findings need to be corroborated in a larger dataset, as only 27 patients provided both baseline and end-of-study samples (CSF collection was optional and a large number of patients were enrolled in countries where willingness among patients to donate CSF is very low). Thus, effect sizes are medium to large, but the confidence intervals are wide. As expected, treatment did not have an effect on amyloid biomarkers in CSF.

The effect on neurodegeneration, documented by CSF tau biomarkers, was also supported by findings in plasma, where AADvac1 reduced the levels of NfL protein. Plasma NfL is an emerging highly responsive marker of the intensity of neurodegeneration[46,47] and was found to be predictive of future cognitive decline in sporadic[29] and familial AD[48]. In addition, plasma NfL concentration correlates with the load of neurofibrillary pathology in the brain, suggesting that NfL in AD may specifically reflect neurodegeneration driven by abnormal tau protein[49]. AADvac1 induced a progressive separation of NfL levels between the AADvac1 and placebo arms. During the study, NfL values in patients on placebo increased at rates reported for patients with AD (ADAMANT, 27.7 %; Alzheimer's Disease Neuroimaging Initiative (ADNI) cohort, ~24%), while levels of AADvac1-treated patients changed at rates usually seen in healthy elderly individuals (ADAMANT, 12.6 %; ADNI cohort, ~14%)[50]. The between-group difference increased progressively with the duration of the treatment to a maximum of 58% difference over 2 years. The investigated fluid biomarkers, tau in the CSF and plasma NfL, can be expected to respond more swiftly to disease-modifying treatments than disease indicators with greater inertia, such as imaging and clinical end points.

Additionally, DTI findings indicate that the vaccine may attenuate white matter degeneration. DTI seems to be a highly sensitive measure of white matter integrity in AD[51]. Specifically, this loss of structure is most likely driven by tau pathology, as healthy tau protein dynamics are essential in maintaining the cytoskeleton and axonal integrity and transport[19,52]; also, similar integrity loss is seen in non-AD tauopathies, such as chronic traumatic encephalopathy[53,54]. The fornix, being a major hippocampal projection, can be expected to manifest these changes early and pronouncedly in AD. Both measures of white matter integrity were stable or showed slight improvement in AADvac1-treated patients, whereas a deterioration was observed in placebo-treated individuals. The differences in FA and MD were statistically significant for the fornix, whereas a trend was observed in the corpus callosum. However, these findings are based on the data available from a small subset of patients and thus need to be interpreted cautiously and confirmed in future clinical development.

There are other limitations of the present study. The sample size calculation was not optimal for the safety evaluation in a parallel group setting, as the original calculation was based on comparing the incidence of AEs in the AADvac1 group to 0. However, post hoc power calculations based on non-inferiority (AADvac1 and placebo difference $\varepsilon = 7\%$, non-inferiority margin $\delta = 15\%$) give a similar power in a parallel-arm setting (162 patients in total to achieve a power of 80%). This affects the study's statistical power, but not the safety assessment itself; the safety analysis remains valid, indicating a benign safety profile of AADvac1. Furthermore, we did not observe direct correlations between the area under the curve (AUC) of antibody response and efficacy outcomes. A likely confounder of this analysis was the high inter-patient variability of the CSF-to-serum ratio of the AADvac1-induced antibodies (0.10–0.58% after 1 year of treatment and 0.16–0.96 % after 2 years of treatment) (Supplementary Table 22). CSF antibody concentration might be used as an approximate measure of antibodies penetrating the blood–brain barrier. The observed high CSF-to-serum ratio variability in patients who underwent lumbar puncture can be expected to be present also in other patients in the study, thus limiting analyses of correlation between the AUC of serum antibodies and cognitive outcomes or MRI. Additionally, we were not able to account for important covariates that can be expected to affect the relationship between antibody response and disease progression, such as the level of seeding-capable tau moieties in the patients' brains, which is also likely to differ between patients[17]. The biomarker data and MRI prediction model indicate that we enrolled a relatively high proportion of patients with non-AD dementia. This points to the need to better stratify patients in future clinical trials by using either PET, blood or CSF biomarkers to target the population with tau pathology and to obtain CSF data in more individuals; a limitation of the present study is that longitudinal CSF biomarker data were available only in a fraction of individuals. Similarly, DTI results are available only for a small subset. Finally, without correcting for multiplicity, the study was powered to detect effect sizes of 0.5 and greater on cognitive and functional outcomes, which corresponds to a ~47% slowing down of decline, as measured by the CDR-SB[55], a rather optimistic assumption. The study was not powered to detect smaller but still-relevant effects (0.2–0.25); this would require a sample size that is utilized in phase 3 AD studies (approximately 700–1,300, depending on power and anticipated dropout).

Together, the preclinical and clinical data support further development of AADvac1. Adequately powered phase 3 studies will be required to attempt to replicate biomarker effects on larger sample sizes and to draw robust conclusions about clinical efficacy of AADvac1.

Methods

Trial design and oversight. The study was conducted at 41 sites in Austria, Czech Republic, Germany, Poland, Romania, Slovakia, Slovenia and Sweden.

The study was a randomized, double-blinded, parallel-arm, placebo-controlled trial.

Following a screening period of up to 6 weeks, patients were randomized between AADvac1 and placebo in a 3:2 ratio and observed for 104 weeks. A safety follow-up was performed 4 weeks after the end-of-study visit (18 weeks after the last dose of treatment). The clinical protocol is available in Supplementary Data 1.

Ethics. All patients and their caregivers provided written informed consent before study procedures. The study complied with the pertinent International Council for Harmonisation of Technical Requirements for Pharmaceuticals for Human Use guidelines and the Declaration of Helsinki. The study was approved by the pertinent ethics committees and competent authorities (see Supplementary Section 2.1 for full list). Study registration details were EudraCT 2015-000630-30 (https://www.clinicaltrialsregister.eu/ctr-search/search?query=AC-AD-003, EudraCT start date 26 November 2015); ClinicalTrials.gov identifier NCT02579252. EudraCT is the official record; the NCT register is incomplete because of author omission.

Period of data collection. First screening: 10 May 2016
First randomization: 16 June 2016
Last end-of-study visit: 25 May 2019
Last safety follow-up: 25 June 2019

Role of the funding source. AXON Neuroscience was involved in the design of the study; in the collection, analysis and interpretation of data; and in the writing of this report. The corresponding author had full access to all data and had final responsibility for submission of the report for publication.

Randomization and treatment masking. Patients were randomized via an interactive web-based response system provided by Cenduit GmbH, Switzerland.

The AADvac1: placebo randomization ratio was 3:2. The randomization block size was 10.

AADvac1 and placebo vials were identical in appearance. Each vial was labeled with a unique identifier code assigned by the independent vendor and the specific vial to be administered to a given patient at a given visit was allocated before administration by the interactive web-based response system.

Patients, caregivers, investigators, outcome assessors and all other personnel involved in trial conduct were blinded to treatment allocation.

Interventions. *Investigational medicinal product and treatment regimen.* Each dose of AADvac1 consisted of 40 µg Axon Peptide 108 (tau 294-305/4R with N-terminal cysteine, amino acid sequence CKDNIKHVPGGGS) coupled to keyhole limpet hemocyanin via a maleimide linker, adjuvanted with aluminum hydroxide (containing 0.5 mg Al^{3+}) in a phosphate buffer volume of 0.3 ml. The design of the vaccine has been described in detail previously[25].

Patients received a total of 11 doses, divided into an initial treatment regimen of 6 doses at 4-week intervals, followed by 5 booster doses administered at 14-week intervals.

The investigational medicinal product (IMP) was injected subcutaneously.

Placebo. Patients assigned to placebo received aluminum hydroxide (containing 0.5 mg Al^{3+}) in a phosphate buffer volume of 0.3 ml.

Eligibility criteria. The study enrolled patients with a diagnosis of probable AD according to the revised National Institute on Aging/Alzheimer's Association criteria[56], an MMSE total score ≥20 and ≤26, a brain MRI consistent with the diagnosis of AD and evidence of the AD pathophysiological process (one or both of the following): (1) medial temporal lobe atrophy on brain MRI (a Scheltens score of ≥2 on a scale of 0–4 on the more atrophied side), (2) positive AD biomarker signature in the CSF (total tau protein >400 pg ml^{-1} and pT181 tau protein >60 pg ml^{-1} and Aβ42 < 600 pg ml^{-1} and Aβ42:Aβ40 ratio <0.089). Patients were aged 50–85 years inclusive. Stable therapy with an acetylcholinesterase inhibitor for at least 3 months before screening was required; memantine treatment was allowed if the dose regimen was stable for at least 3 months before screening.

Excluded from participation were patients with central nervous system disorders other than AD that could be the cause of dementia; immunodeficiency, clinically relevant autoimmune disease, current or expected immunosuppressive or immunomodulatory treatment; MRI abnormalities such as infarction in the territory of large vessels, more than one lacunar infarct or any lacunar infarct in a strategically important location, confluent hemispheric deep white matter lesions (Fazekas grade 3) or other focal lesions that may be responsible for the cognitive status of the patient; severe comorbidities such as recent cancer, recent myocardial infarction, poorly controlled diabetes, poorly controlled congestive heart failure, severe renal insufficiency, relevant psychiatric illness, epilepsy, chronic liver disease, chronic infectious disease (hepatitis B, hepatitis C, HIV or syphilis); uncorrected hypothyroidism or B12 hypovitaminosis.

See Supplementary Section 3 for full verbatim listing of eligibility criteria.

End points and objectives. *Primary end point.* Safety. Pre-specified analysis encompassed the comparison of overall incidence of AEs and SAEs between the AADvac1 and placebo arm and the comparisons of AE incidence for each SOC. A separate analysis was pre-specified for expected ISRs. Post hoc comparisons at the preferred term (PT) level were performed where suggested by the DSMB.

Reports of AEs were obtained by nondirective questioning from patients and their caregivers and by reviewing the patient's diary. A structured neurological and physical examination was conducted by the investigators at each visit. Vital signs were assessed at every visit and 1 h after AADvac1 administration. Standard laboratory panels (biochemistry, coagulation, hematology) and dipstick urinalysis were performed at each visit. Investigators reported clinically relevant abnormalities as AEs.

A standard ECG was performed at screening and weeks 12, 24, 52, 80 and 104.

Safety MRIs were performed at 6-month intervals and each scan was assessed in parallel by the investigator and the Sponsor's radiologist. A manual review of all MRIs was performed by the Sponsor to quantify the incidence of MHs in all patients who had a post-baseline MRI (AADvac1 $n=114$, placebo $n=75$).

Accruing safety data were reviewed approximately every 6 months by an independent DSMB.

Secondary end points. Mean change in CDR-SB score over 104 weeks; mean change in CCB composite *z* score over 104 weeks; mean ADCS-MCI-ADL score over 104 weeks; and geometric mean antibody response at each post-baseline visit.

Exploratory and research end points and objectives. The exploratory and research end points and objectives are as follows. Mean change in CSF biomarkers from baseline to week 104; mean change in hippocampal volume, entorhinal cortex volume, whole brain volume and a range of other regions of interest from screening to week 104; mean change in brain metabolism as measured by fluorodeoxyglucose PET over 104 weeks; mean change in individual domains of cognition of the CCB from baseline to week 104; mean change in MMSE score from screening to week 104; correlation between AUC of IgG antibody titer to Axon Peptide 108 and change in efficacy and biomarker assessments; mean change in white matter integrity measured by DTI MRI in the fornix and CC (genu, body and splenium) from screening to week 104; mean change in blood biomarkers (proline-rich region containing tau, N-terminal tau, NfL chain protein) from baseline to week 104; change in functional brain connectivity as measured by resting state functional MRI from screening to week 104; immunological characterization of vaccine responders; evaluation of phenotype of the immune response to AADvac1 using flow cytometry of cellular markers, cytokine profiling and immune marker quantitative PCR with reverse transcription.

Assessments not reported in this manuscript. A subset of results of the study are not reported in this manuscript.

The fluorodeoxyglucose PET assessment could not be evaluated due to technical difficulties. The number of recorded functional MRI sequences was too low to evaluate (the sequence was optional). The planned N-terminal CSF tau assay specified in the protocol was not performed, as during assay optimization it was realized that it does not discriminate between AD and healthy controls and therefore does not reflect tau pathology in the brain. The assays for proline-rich regions containing tau and N-terminal tau in the plasma could not be optimized in time. The latter also does not seem to reflect brain tau pathology. The details on immunological characterization would exceed the scope of the present manuscript.

Sample size calculation. An overall dropout rate of 25% was assumed. Sample sizes were increased to correct for dropout. Dropouts were not to be replaced.

For the primary objective (safety assessment). The study was powered to detect an AE with an incidence of 7% and higher. At least 83 individuals on AADvac1 treatment were required to complete the study to show an AE incidence of 7% and higher as statistically significant with a power of 0.80 at the significance level of 0.05, using a one-sided one-sample Wald *z*-test (H_0, incidence is equal to zero; H_1, incidence is not equal to zero). Correcting for 25% dropout, at least 111 individuals would need to be enrolled and randomized in the AADvac1 arm.

Given a 3:2 AADvac1 to placebo allocation, at least 55 individuals on placebo treatment were required to complete the study. Correcting for 25% dropout and given a 3:2 AADvac1 to placebo allocation, at least 74 individuals needed to be enrolled and randomized in the placebo arm.

A non-inferiority post hoc power calculation was also undertaken. With a 15% non-inferiority margin, a trial with 97 individuals on AADvac1 and 65 on placebo (162 patients in total) has 80% power in a one-sided non-inferiority test at the significance level of 0.1, to demonstrate non-inferiority of AADvac1 to placebo with respect to incidence of AEs if AADvac1 has a 7% higher incidence of AEs compared to placebo; using a two-sample Wald *z*-test with adjustment according to[57] (H_0, the incidence of AEs in AADvac1 minus placebo ≥0.15; H_1, the incidence of AEs in AADvac1 minus placebo <0.15).

With 111 patients enrolled in the AADvac1 group and 83 patients on AADvac1 treatment expected to complete the 2-year trial, 194 patient-years of on-treatment safety data were to be generated (assuming linear dropout). Given this dataset, the study had a >95% chance to observe at least one occurrence of hypothetical AEs with a true annual incidence of 1:65 or higher (derived from 3 of 194 based on the approximation of upper confidence level of one-sided 95% CI by a rule of three).

For the secondary clinical and cognitive end points. The majority of the secondary end points are efficacy end points relating to the assessments of cognitive decline. Given a 3:2 AADvac1 to placebo allocation, at least 135 individuals (81:54) were expected to be required to complete the trial to show a standardized difference of 0.5 as statistically significant with a power of 0.80 and at the significance level of 0.05 using a two-sided two-sample Student *t*-test. On the CDR-SB, an effect size of 0.5 would correspond to a 47% slowing of patient decline over 2 years[55].

Correcting for a 25% dropout and given a 3:2 AADvac1 to placebo allocation, 180 individuals (108:72) would need to be randomized in the study.

No sample size calculations were performed for exploratory end points.

Measurement of titers of antibodies against Axon Peptide 108. The titers of vaccine-induced antibodies were determined using serially diluted serum samples with indirect ELISA by a validated method with a range from 1:100 to 1:204,800 serum dilution, performed at a clinical biochemistry laboratory fully blinded to sample identity and treatment allocation. Axon Peptide 108 was immobilized on microtiter plates (High-Binding strip plates, Greiner Bio One) at a final concentration of 5 µg ml^{-1}. After blocking with PBS-0.075% Tween 20 for 1 h at 25 °C, plates were incubated overnight at 4 °C with serially diluted serum samples of patients. After washing, bound antibodies were detected using anti-human immunoglobulins (IgG) conjugated to horseradish peroxidase, diluted 1:5,000 in PBS-0.075% Tween 20 (Thermo Fisher Scientific). The amount of bound secondary antibodies was detected with the chromogenic substrate TMB One (KEM-EN-TEC Diagnostic). The resulting signal was compared to that obtained for the patient's serum collected at baseline. The titer of the antibodies in the serum as the highest dilution at which the absorbance at 450 nm was defined at least twice the absorbance of equally diluted pre-immunization serum samples. To ensure assay consistency and quality, we used quality control samples with

two concentrations (13.3 ng ml^{-1} and 1.33 ng ml^{-1}) of the humanized version of monoclonal antibody DC8E8 (AX004) on all plates.

Quantitative ELISA for antibodies to Axon Peptide 108. The amount of human antibodies specific to Axon Peptide 108 was determined using quantitative ELISA. The quantification range was from 300 pg ml^{-1} to 24 ng ml^{-1}; dilutional linearity within the required working range was validated. Axon Peptide 108 was immobilized on microtiter plates (High- Binding strip plates, Greiner Bio One) at a final concentration of 5 µg ml^{-1} and incubated at 37 °C for 2 h. AX004 standard was diluted in standard diluent (normal human serum (IPLA-SER, Innovative Research Inc.) diluted 2,000× in PBS-0.075% Tween 20, 0.05 % BSA and 0.01 % casein) in serial 2.3-fold dilutions starting from 50 ng ml^{-1}, followed by 21.74; 9.452; 4.109; 1.787; 0.777; 0.338 and 0.147 ng ml^{-1}. Then, after blocking with PBS-0.075% Tween 20 for 1 h at 25 °C, 50 µl per well of each dilution of standard, serum samples 2,000× diluted in sample diluent (PBS-0.075% Tween 20, 0.05 % BSA and 0.01 % casein) negative control (standard diluent) and blank (sample diluent) were added into the plate with immobilized peptide and incubated overnight at 4 °C. After washing, bound antibodies were detected with anti-human immunoglobulins (IgG) conjugated to horseradish peroxidase, diluted 1:5,000 in PBS-0.075% Tween 20 (Thermo Fisher Scientific) using chromogenic substrate TMB One (KEM-EN-TEC Diagnostic). Then, evaluation of results was performed using GraphPad Prism software.

Antibodies used in this study. *Primary antibodies.* Primary antibodies used were as follows. AX004, targeting tau assembly-regulating domains in MTBR region, by AXON Neuroscience, patent WO2016079597A1 (refs. [23,24]). DC2E7, targeting tau phospho-threonine pT217, by AXON Neuroscience, patent WO 2019/186276 A2. 2019-10-03 (ref. [43]). DC2E2, targeting tau 164-174, by AXON Neuroscience, patent WO 2019/186276 A2. 2019-10-03 (ref. [43]).

Secondary antibodies. Secondary antibodies used were as follows. Goat anti-human IgG (H+L); secondary antibody, HRP conjugate, cat. no. 31410, lot no. QE2020434 (Thermo Fisher Scientific).

Fluid biomarker measurements. Concentrations of NfL in human plasma and p-tau T217 in CSF were measured using single molecule array (Simoa) digital ELISA, using an HD-1 Analyzer (Quanterix). For the analysis either Simoa NF-Light Advantage kit (Quanterix) or the newly developed and validated p-tau T217 assay[43] were used. Each measurement was performed in duplicate according to manufacturer recommendations. Concentrations were calculated using Simoa HD-1 instrument software v.1.5.

Concentrations of t-tau and p-tau T181 in CSF were measured by Innotest ELISA assays (Fujirebio).

Cognitive, clinical and functional assessments. A standard CDR scale, the ADCS-MCI-ADL 24-item scale and CCB were assessed at 3-month intervals. The CCB consisted of CogState computerized tests (International Shopping List task immediate and delayed recall and recognition, One-Card Learning and One-Card Back)[58–60] and paper-and-pencil tests (Category Fluency: animals, Letter Fluency and Digit Symbol Coding). For the International Shopping List task, 12 words were presented, with three learning rounds for immediate recall and one free delayed recall trial. In the recognition step, these were presented with 12 confounder words. The Letter Fluency and Category Fluency tests had a time limit of 60 s per trial. Three trials were performed for the Letter Fluency Test, with letters selected according to their frequency as starting letters of words in the respective languages. For the International Shopping List test, words were similarly selected according to frequency of their appearance as shopping list items in the respective countries. The Digit Symbol Coding test had a time limit of 120 s.

MMSE was completed at screening, week 12, week 52 and week 104.

Computerized versions of the CDR, ADCS-MCI-ADL and MMSE were performed on the MedAvante Virgil platform.

MRI (volumetry and DTI). The MRI scans performed at each assessment included:

- one or two combined scout scans (T1-weighted axial scout, T1-weighted coronal scout, T1-weighted sagittal scout),
- an axial T2-weighted sequence,
- an axial FLAIR sequence,
- an axial T2*-weighted scan,
- a sagittal T1-weighted three-dimensional (3D) scan,
- an optional diffusion-weighted sequence.

The scout scans served for exact repositioning in the follow-up examinations. The FLAIR and T2-weighted scans served to assess white matter changes and to check for conformity to inclusion criteria. The T2*-weighted gradient sequence served to detect MHs. The sagittal 3D T1-weighted scan was used for assessing brain atrophy, including loss of hippocampal and cortical volume.

Volumetric analysis was performed for the following regions of interest: total brain, hippocampus (left and right), lateral ventricles, basal ganglia, entorhinal cortex (left and right), whole cortex and frontal, temporal, parietal and occipital cortex.

Whole brain volume loss was calculated with SIENA 2.6 (part of FMRIB Software Library (FSL), Oxford Centre for Functional MRI of the Brain). Anatomical locations were determined from automated labeling with FreeSurfer. To extract volume estimates of individual regions of interest, images were automatically processed with the longitudinal stream[61] in FreeSurfer (v.6.0). Specifically, an unbiased within-individual template space and image was created using robust, inverse consistent registration[62]. Several processing steps, such as skull stripping, Talairach transforms, atlas registration as well as spherical surface maps and parcellations were then initialized with common information from the within-individual template, pronouncedly increasing reliability and statistical power[61].

Image processing of the diffusion-weighted scans was conducted with tools from FSL 6.0 (FSL, Oxford). Following eddy current correction and brain extraction, the diffusion tensor was estimated from the diffusion-weighted scans with DTIFIT. To assess the FA and MD in the fornix and in the genu, body and splenium of the CC, regional masks were taken from the FreeSurfer segmentation. This required the nonlinear registration of FA maps to the T1-weighted MPRAGE scan with FNIRT. The resulting transformation matrix then was also applied to the MD maps. Masks were visually checked and manually corrected in case of segmentation errors.

Field strength was 3T. Area of acquisition was the whole brain. Parameters were as follows: T2 FLAIR (TR/TI/TE = 10,000/2,600/100–120 ms, slice thickness of 5 mm, slice gap of 0 mm, field of view of 240 mm, matrix of 256 × 256); T2 TSE (TR/TE = 2,000–4,000/80–120 ms, slice thickness of 5 mm, slice gap of 0 mm, field of view of 240 mm, matrix of 256 × 256); T2* gradient echo (TR/TE = 600–700/20 ms, flip angle of 20°, slice thickness of 5 mm, slice gap of 0 mm, field of view of 240 mm, matrix of 256 × 256); and T1W 3D (MPRAGE or T1-TFE, 1 mm isotropic resolution with whole brain coverage). Diffusion MRI parameters: TR = 7 s, TE = 80–100 ms, 41 diffusion directions with $b = 1{,}000$ s mm^{-2}, five repeats of $b = 0$ s mm^{-2}, 2.7-mm isotropic resolution, single-shot echo planar imaging readout with SENSE/GRAPPA factor of 2–3. 3D T1 scans were normalized by nonlinear registration to a template. Diffusion-weighted scans were registered through corresponding 3D T1 scans and by using the *b*0 scan as reference. The obtained transformation matrix then was applied to the entire diffusion-weighted ($b = 1{,}000$ s mm^{-2}) series. The normalization template was MNI305. All scans that were affected by noise and motion artifacts were repeated or excluded from analysis. No volume censoring was performed.

MRI-based multimodal classifier. A newly available methodology developed by Tosun and colleagues was employed for assessing brain Aβ-positivity and tau-positivity status of ADAMANT participants[31,32,35]. This approach used 5,000+ ADNI structural MRI scans with known Aβ-positivity status based on either CSF or PET imaging and tau-positivity status based on CSF p-tau together with demographics data (age, sex, years of education and *APOE* genotype) and CDR-SB score at the screening visit to train a deep-learning (DL) model. The fully trained DL model was first independently tested on a validation cohort of 340 ADNI patients with mild-to-moderate AD, aged between 54 and 85 years, followed by a final independent validation in a subset of ADAMANT participants who had CSF biomarker assessment at the screening visit. The method yields individual-level probabilistic scores between 0 and 1 for Aβ-positivity and tau-positivity, with values ≥0.5 interpreted as $A\beta^+$ and tau^+. The $A\beta^+$ versus $A\beta^-$ discrimination accuracy of the DL model in the independent validation cohort of ADAMANT CSF substudy was 93% with 98% positive predictive value. In the same ADAMANT CSF substudy cohort, the tau^+ versus tau^- discrimination accuracy of the DL model was 83% with 96% positive predictive value. These models were used to estimate Aβ and tau status of participants in the ADAMANT study using MRI, demographics and CDR-SB data acquired at the screening visit.

CONSORT 2010 details and supplementary data are located in Supplementary Information.

Statistical methods. We performed statistical analyses using the R programming environment v.4.0.5 (R Development Core Team 2020) and GraphPad Prism v.8.3.1 (GraphPad Software). For ANCOVA pre-specified in the statistical analysis plan (SAP) we used SAS software (SAS Proprietary Software 9.4 (TS1M5)). All alternative hypotheses were two-sided and statistical tests were performed at a significance level equal to 0.05. Additional safety alternative hypotheses associated with non-inferiority were one sided and statistical tests were performed at a significance level equal to 0.1. Analyses of incidence of AEs were performed on the safety set; all other analyses were conducted on the FAS. All *P* values and confidence intervals are reported without correction for multiplicity; where applicable, the number of statistical comparisons is listed.

Due to the high background incidence of AEs in elderly patients with AD, the safety analysis was a comparison of whether the AE was significantly more common than in the placebo group using Wald two-sample *z*-test as defined in the SAP (see combined protocol/SAP Supplementary Information). As an effect, the incidence of relative risk of AADvac1 to placebo was calculated. The null hypotheses that log relative risk is equal to one were tested against two-sided

alternative by two-sample Wald *z*-test statistic[63]. The boundaries of empirical two-sided Wald 95% CIs for relative risk were calculated by the back transformation from log relative risk scale to relative risk scale. The log relative risk scale was used as this was a variance stabilizing transformation of the relative risk scale.

For the overall number of individuals with TEAEs, as well as individuals with TEAEs in each SOC, a logistic regression analysis was applied to examine whether there is an association between TEAEs and treatment as defined in the SAP. The logistic regression analysis was performed if at least 5% of individuals reported the event. The logistic regression model included treatment group, pooled country and sex as factors, as well as age as a continuous covariate and was used to estimate the odds ratio for treatment (AADvac1 versus placebo) and associated two-sample Wald test *P* value. (H_0, odds ratio of incidence is equal to one; two-sided H_1, odds ratio of incidence is not equal to one).

Additional safety analyses were performed using a two-sample Wald *z*-test of non-inferiority with adjustment[57] and risk difference was reported together with the upper bound of an empirical one-sided Wald 90% CI for risk difference (this was compared to a non-inferiority margin of $\delta = 15\%$; H_0, the incidence of AEs in AADvac1 minus placebo $\geq \delta$; H_1, the incidence of AEs in AADvac1 minus placebo $< \delta$).

The incidence of events such as reversible ISRs and MHs was calculated as follows:

1. Reversible ISRs: 1, patient with at least one reversible ISR on any post-baseline visit; 0, patient with no reversible ISR on any post-baseline visit.
2. MHs: 1, patient with post-screening MRIs (including early discontinuation visit) and at least on one of them with more MHs than at screening or new MHs; 0, patient with post-screening MRIs (including early discontinuation visit) and on none of them with more MHs that at screening or no new MHs; NA, patient without post-screening MRIs.

Antibody response variables, such as serum IgG antibody titer to Axon Peptide 108 and serum IgG antibody titer to Axon Peptide 108 measured by quantitative ELISA, were lognormally distributed (as tested by Lilliefors goodness-of-fit test)[64], therefore the geometric mean instead of mean was estimated for AADvac1. Additionally, the boundaries of two-sided empirical Wald 95% CI for geometric mean were calculated. The data, geometric means and 95% CIs were calculated and visualized using box plots at each post-baseline visit.

Plasma NfL, CSF tau markers (CSF t-tau, CSF p-tau pT181, CSF p-tau pT217, CSF Aβ42, CSF Aβ40 and CSF neurogranin) and DTI variables (fractional anisotropy of the fornix, mean diffusivity of the fornix, FA of the genu of the corpus callosum and MD of the genu of the CC) data were winsorised per study arm using Tukey IQR approach due to the presence of outliers. For plasma NfL and CSF tau markers, winsorisation was conducted for differences from baseline. For DTI variables, the winsorisation was performed for differences from screening. MRI volumetry data (total cortex volume, temporal cortex volume, lateral ventricles volume, whole brain volume and total hippocampal volume as sum of left and right) used as percentual change from screening were winsorised using 2.5% and 97.5% percentiles on joint data from both study arms.

In the case of CSF tau markers, visits were pulled together before winsorisation as follows, V01 and V02; V11 and V14A; and V15 and V16. For further statistical analyses, the difference of V16 (week 104) and baseline was used. For plasma NfL, mean change and empirical two-sided Wald 95% CI for mean change using two-sample Student *t*-test approach for AADvac1 and placebo were calculated. The nullity of differences in means between AADvac1 and placebo were assessed using a two-sample Student *t*-test with Welch approximation of degrees of freedom[65] and results are reported as *t*-statistics, degrees of freedom, mean difference and empirical two-sided Wald 95% CI for mean difference. Additionally, the effect size Cohen's *d* and its empirical Wald 95% CI was calculated using variance stabilizing transformation[66] (chapter 5, B2).

To visualize the distribution of plasma NfL at baseline, box plots were used. For CSF tau markers, means per AADvac1 and placebo together with Cohen's *d* and its empirical two-sided Wald 95% CI were calculated. Changes from baseline of plasma NfL and CSF tau markers were visualized as mean profiles with 95% CIs per study arm. CSF tau markers were also visualized as temporal profiles of all patients together with mean profiles per study arm.

For DTI variables, Cohen's *d* and its empirical two-sided Wald 95% CI was calculated. Changes from screening were visualized as mean profiles with empirical two-sided Wald 95% CIs for means per study arm, as data temporal profiles of all patients together with mean profiles per study arm.

All *P* values are reported without correction for multiplicity. Where relevant, the number of performed comparisons is reported.

MMRM. MMRM analysis including all post-dose results assigned to scheduled visit weeks (excluding unscheduled visits) was used to analyze change from baseline. No imputation was required before MMRM. The MMRM model included fixed-effect terms for treatment group, visit, pooled country, sex, age, years of education, *APOE4* status, baseline MRI hippocampal volume and baseline CDR-SB. The interaction term between treatment group and visit was also included to allow the treatment group difference to change over time. The visit is the repeated measure on individuals in this model, which was modeled in PROC MIXED in SAS using the REPEATED statement. The variance–covariance matrix was assumed to be unstructured. From this model, the LS mean treatment difference (AADvac1 − placebo) at week 104 (V16) was calculated along with the 95% CI and the two-sided *P* value for treatment comparison.

ANCOVA. All ANCOVA models were specified on dependent variables defined as a change from baseline or screening (as applicable) to week 104.

In pre-specified ANCOVA models on FAS for CDR-SB, CCB composite *z*-scores and ADCS-MCI-ADL 24 as dependent variables, the following covariates were included in the ANCOVA model: sex, *APOE4* status, age (AGE), planned treatment group (TRTP), baseline CDR-SB score (BASECDR), background AD therapy (either AChEI alone or AChEI and memantine combination therapy (ADTHER)), years of formal education (EDUCATION), baseline hippocampus volume (BASEMRI) and pooled country (pooled Sweden, Germany and Austria versus pooled Czech Republic, Slovakia, Slovenia, Poland and Romania (PCOUNTRY)).

TRTP and BASECDR were forced into the model. For the CCB and ADCS-MCI-ADL, the baseline value of the respective assessment was also forced into the model (BASECCB and BASEADL). Interaction terms are denoted with * (Supplementary Tables 23–25).

Stepwise selection was performed with the stopping rule based on *P* values with a significance level equal to 0.10 (ref. [67]). In the ANCOVA models on the algorithm-defined A^+T^+ group for CDR-SB, MMSE score, ADCS-MCI-ADL 24 score, plasma NfL, total cortex volume (%), temporal cortex volume (%), total hippocampal volume (%) and lateral ventricles volume (%), the following covariates were included in the model: baseline value of the given assessment, age and baseline plasma NfL. The results are reported as adjusted mean difference, empirical two-sided Wald 95% CI of adjusted mean difference and adjusted *P* value.

In the ANCOVA models for plasma NfL, CSF tau markers and MRI volumetry data, the baseline value of each given biomarker was included as a covariate. The results are reported as adjusted mean difference, empirical Wald 95% CI of adjusted mean difference and adjusted *P* value.

Reporting Summary. Further information on research design is available in the Nature Research Reporting Summary linked to this article.

Data availability

Raw data for figures are available as supplementary materials.
The data that support the findings of this study are available from the corresponding author upon reasonable request.
Antibodies utilized in this study are available from the corresponding author upon reasonable request.

Code availability

The R-code is deposited on GitHub: https://doi.org/10.5281/zenodo.3862685.

Received: 9 November 2020; Accepted: 28 April 2021;

References

1. Braak, H. & Braak, E. Neuropathological stageing of Alzheimer-related changes. *Acta Neuropathol.* **82**, 239–259 (1991).
2. Wischik, C. M. et al. Isolation of a fragment of tau derived from the core of the paired helical filament of Alzheimer disease. *Proc. Natl Acad. Sci. USA* **85**, 4506–4510 (1988).
3. Grundke-Iqbal, I. et al. Abnormal phosphorylation of the microtubule-associated protein tau (tau) in Alzheimer cytoskeletal pathology. *Proc. Natl Acad. Sci. USA* **83**, 4913–4917 (1986).
4. Whitwell, J. L. et al. Neuroimaging correlates of pathologically defined subtypes of Alzheimer's disease: a case-control study. *Lancet Neurol.* **11**, 868–877 (2012).
5. Nelson, P. T. et al. Correlation of Alzheimer disease neuropathologic changes with cognitive status: a review of the literature. *J. Neuropathol. Exp. Neurol.* **71**, 362–381 (2012).
6. Murray, M. E. et al. Clinicopathologic and 11C-Pittsburgh compound B implications of Thal amyloid phase across the Alzheimer's disease spectrum. *Brain* **138**, 1370–1381 (2015).
7. La Joie, R. et al. Prospective longitudinal atrophy in Alzheimer's disease correlates with the intensity and topography of baseline tau-PET. *Sci. Transl. Med.* https://doi.org/10.1126/scitranslmed.aau5732 (2020).
8. Mattsson-Carlgren, N. et al. The implications of different approaches to define AT(N) in Alzheimer disease. *Neurology* **94**, e2233–e2244 (2020).
9. Braak, H. & Del Tredici, K. The pathological process underlying Alzheimer's disease in individuals under thirty. *Acta Neuropathol.* **121**, 171–181 (2011).
10. Franzmeier, N. et al. Functional brain architecture is associated with the rate of tau accumulation in Alzheimer's disease. *Nat. Commun.* **11**, 347 (2020).

11. Vasili, E., Dominguez-Meijide, A. & Outeiro, T. F. Spreading of α-synuclein and tau: a systematic comparison of the mechanisms involved. *Front. Mol. Neurosci.* **12**, 107 (2019).
12. Zilka, N., Korenova, M. & Novak, M. Misfolded tau protein and disease modifying pathways in transgenic rodent models of human tauopathies. *Acta Neuropathol.* **118**, 71–86 (2009).
13. Rauch, J. N. et al. LRP1 is a master regulator of tau uptake and spread. *Nature* **580**, 381–385 (2020).
14. Holmes, B. B. et al. Heparan sulfate proteoglycans mediate internalization and propagation of specific proteopathic seeds. *Proc. Natl Acad. Sci. USA* **110**, E3138–E3147 (2013).
15. Mudher, A. et al. What is the evidence that tau pathology spreads through prion-like propagation? *Acta Neuropathol. Commun.* **5**, 99 (2017).
16. Colin, M. et al. From the prion-like propagation hypothesis to therapeutic strategies of anti-tau immunotherapy. *Acta Neuropathol.* **139**, 3–25 (2020).
17. Aoyagi, A. et al. Aβ and tau prion-like activities decline with longevity in the Alzheimer's disease human brain. *Sci. Transl. Med.* https://doi.org/10.1126/scitranslmed.aat8462 (2019).
18. Brunello, C. A. et al. Mechanisms of secretion and spreading of pathological tau protein. *Cell. Mol. Life Sci.* **77**, 1721–1744 (2020).
19. Jadhav, S. et al. A walk through tau therapeutic strategies. *Acta Neuropathol. Commun.* **7**, 22 (2019).
20. Congdon, E. E. & Sigurdsson, E. M. Tau-targeting therapies for Alzheimer disease. *Nat. Rev. Neurol.* **14**, 399–415 (2018).
21. Dingman, R. & Balu-Iyer, S. V. Immunogenicity of protein pharmaceuticals. *J. Pharm. Sci.* **108**, 1637–1654 (2019).
22. Kontsekova, E. et al. Identification of structural determinants on tau protein essential for its pathological function: novel therapeutic target for tau immunotherapy in Alzheimer's disease. *Alzheimers Res. Ther.* **6**, 45 (2014).
23. Weisova, P. et al. Therapeutic antibody targeting microtubule-binding domain prevents neuronal internalization of extracellular tau via masking neuron surface proteoglycans. *Acta Neuropathol. Commun.* **7**, 129 (2019).
24. Zilkova, M. et al. Humanized tau antibodies promote tau uptake by human microglia without any increase of inflammation. *Acta Neuropathol. Commun.* https://doi.org/10.1186/s40478-020-00948-z (2020).
25. Kontsekova, E. et al. First-in-man tau vaccine targeting structural determinants essential for pathological tau–tau interaction reduces tau oligomerisation and neurofibrillary degeneration in an Alzheimer's disease model. *Alzheimers Res. Ther.* **6**, 44 (2014).
26. Novak, P. et al. Safety and immunogenicity of the tau vaccine AADvac1 in patients with Alzheimer's disease: a randomised, double-blind, placebo-controlled, phase 1 trial. *Lancet Neurol.* **16**, 123–134 (2017).
27. Novak, P. et al. FUNDAMANT: an interventional 72-week phase 1 follow-up study of AADvac1, an active immunotherapy against tau protein pathology in Alzheimer's disease. *Alzheimers Res. Ther.* **10**, 108 (2018).
28. Fagerland, M. W., Lydersen, S. & Laake, P. Recommended confidence intervals for two independent binomial proportions. *Stat. Methods Med. Res.* **24**, 224–254 (2015).
29. de Wolf, F. et al. Plasma tau, neurofilament light chain and amyloid-β levels and risk of dementia; a population-based cohort study. *Brain* **143**, 1220–1232 (2020).
30. Lang, A., Weiner, M. W. & Tosun, D. O4-04-01: what can structural MRI tell about A/T/N staging? *Alzheimers Dement.* **15**, P1237–P1238 (2019).
31. Tosun, D. et al. Neuroimaging predictors of brain amyloidosis in mild cognitive impairment. *Ann. Neurol.* **74**, 188–198 (2013).
32. Tosun, D. et al. Multimodal MRI-based imputation of the $A\beta^{+}$ in early mild cognitive impairment. *Ann. Clin. Transl. Neurol.* **1**, 160–170 (2014).
33. Bateman, R. J. et al. The DIAN-TU next generation Alzheimer's prevention trial: adaptive design and disease progression model. *Alzheimers Dement.* **13**, 8–19 (2017).
34. Gordon, B. A. et al. Tau PET in autosomal dominant Alzheimer's disease: relationship with cognition, dementia and other biomarkers. *Brain* **142**, 1063–1076 (2019).
35. Tosun, D. et al. Amyloid status imputed from a multimodal classifier including structural MRI distinguishes progressors from nonprogressors in a mild Alzheimer's disease clinical trial cohort. *Alzheimers Dement.* **12**, 977–986 (2016).
36. Grubeck-Loebenstein, B. et al. Immunosenescence and vaccine failure in the elderly. *Aging Clin. Exp. Res.* **21**, 201–209 (2009).
37. Albert, M. et al. Prevention of tau seeding and propagation by immunotherapy with a central tau epitope antibody. *Brain* **142**, 1736–1750 (2019).
38. Yanamandra, K. et al. Anti-tau antibodies that block tau aggregate seeding in vitro markedly decrease pathology and improve cognition in vivo. *Neuron* **80**, 402–414 (2013).
39. Jack, C. R. Jr. et al. NIA-AA research framework: toward a biological definition of Alzheimer's disease. *Alzheimers Dement.* **14**, 535–562 (2018).
40. Molinuevo, J. L. et al. Current state of Alzheimer's fluid biomarkers. *Acta Neuropathol.* **136**, 821–853 (2018).
41. Janelidze, S. et al. Cerebrospinal fluid p-tau217 performs better than p-tau181 as a biomarker of Alzheimer's disease. *Nat. Commun.* **11**, 1683 (2020).
42. Barthelemy, N. R. et al. Cerebrospinal fluid phospho-tau T217 outperforms T181 as a biomarker for the differential diagnosis of Alzheimer's disease and PET amyloid-positive patient identification. *Alzheimers Res. Ther.* **12**, 26 (2020).
43. Hanes, J. et al. Evaluation of a novel immunoassay to detect p-Tau Thr217 in the CSF to distinguish Alzheimer's disease from other dementias. *Neurology* https://doi.org/10.1212/WNL.0000000000010814 (2020).
44. Palmqvist, S. et al. Discriminative accuracy of plasma phospho-tau217 for Alzheimer disease vs other neurodegenerative disorders. *JAMA* https://doi.org/10.1001/jama.2020.12134 (2020).
45. Nelson, P. T. et al. Limbic-predominant age-related TDP-43 encephalopathy (LATE): consensus working group report. *Brain* https://doi.org/10.1093/brain/awz099 (2019).
46. Rohrer, J. D. et al. Serum neurofilament light chain protein is a measure of disease intensity in frontotemporal dementia. *Neurology* **87**, 1329–1336 (2016).
47. Benedet, A. L. et al. Plasma neurofilament light associates with Alzheimer's disease metabolic decline in amyloid-positive individuals. *Alzheimers Dement.* **11**, 679–689 (2019).
48. Preische, O. et al. Serum neurofilament dynamics predicts neurodegeneration and clinical progression in presymptomatic Alzheimer's disease. *Nat. Med.* **25**, 277–283 (2019).
49. Ashton, N. J. et al. Increased plasma neurofilament light chain concentration correlates with severity of post-mortem neurofibrillary tangle pathology and neurodegeneration. *Acta Neuropathol. Commun.* **7**, 5 (2019).
50. Mattsson, N. et al. Association between longitudinal plasma neurofilament light and neurodegeneration in patients with Alzheimer disease. *JAMA Neurol.* **76**, 791–799 (2019).
51. Strain, J. F. et al. Loss of white matter integrity reflects tau accumulation in Alzheimer disease defined regions. *Neurology* **91**, e313–e318 (2018).
52. Mephon-Gaspard, A. et al. Role of tau in the spatial organization of axonal microtubules: keeping parallel microtubules evenly distributed despite macromolecular crowding. *Cell. Mol. Life Sci.* **73**, 3745–3760 (2016).
53. Ng, T. S. et al. Neuroimaging in repetitive brain trauma. *Alzheimers Res. Ther.* **6**, 10 (2014).
54. Holleran, L. et al. Axonal disruption in white matter underlying cortical sulcus tau pathology in chronic traumatic encephalopathy. *Acta Neuropathol.* **133**, 367–380 (2017).
55. Cedarbaum, J. M. et al. Rationale for use of the clinical dementia rating sum of boxes as a primary outcome measure for Alzheimer's disease clinical trials. *Alzheimers Dement.* **9**, S45–S55 (2013).
56. McKhann, G. M. et al. The diagnosis of dementia due to Alzheimer's disease: recommendations from the national institute on aging-Alzheimer's association workgroups on diagnostic guidelines for Alzheimer's disease. *Alzheimers Dement.* **7**, 263–269 (2011).
57. Agresti, A. & Caffo, B. Simple and effective confidence intervals for proportions and differences of proportions result from adding two successes and two failures. *Am. Stat.* **54**, 280–288 (2000).
58. Baker, J. E. et al. Episodic memory and learning dysfunction over an 18-month period in preclinical and prodromal Alzheimer's disease. *J. Alzheimers Dis.* **65**, 977–988 (2018).
59. Grove, R. A. et al. A randomized, double-blind, placebo-controlled, 16-week study of the H3 receptor antagonist, GSK239512 as a monotherapy in subjects with mild-to-moderate Alzheimer's disease. *Curr. Alzheimer Res.* **11**, 47–58 (2014).
60. Scheltens, P. et al. Safety, tolerability and efficacy of the glutaminyl cyclase inhibitor PQ912 in Alzheimer's disease: results of a randomized, double-blind, placebo-controlled phase 2a study. *Alzheimers Res. Ther.* **10**, 107 (2018).
61. Reuter, M. et al. Within-subject template estimation for unbiased longitudinal image analysis. *Neuroimage* **61**, 1402–1418 (2012).
62. Reuter, M., Rosas, H. D. & Fischl, B. Highly accurate inverse consistent registration: a robust approach. *Neuroimage* **53**, 1181–1196 (2010).
63. Katz, D. et al. Obtaining confidence intervals for the risk ratio in cohort studies. *Biometrics* **34**, 469–474 (1978).
64. Lilliefors, H. W. On the Kolmogorov–Smirnov test for normality with mean and variance unknown. *J. Am. Stat. Assoc.* **62**, 399–402 (1967).
65. Welch, B. L. The generalization of 'Student's' problem when several different population variances are involved. *Biometrika* **34**, 28–35 (1947).
66. Hedges, L. V. & Olkin, I. *Statistical Methods for Meta-analysis*. Ch. 5, B2 (Academic Press, 1985).
67. Chowdhury, M. Z. I. & Turin, T. C. Variable selection strategies and its importance in clinical prediction modelling. *Fam. Med. Community Health* **8**, e000262 (2020).

Acknowledgements

The study was funded by AXON Neuroscience SE. The authors thank the patients and their caregivers and the ADAMANT investigators (Supplementary Section 13).

Author contributions

P.N. developed the study design and SAP, performed data analysis and interpretation and manuscript preparation. B.K. led investigational medicinal product (IMP) design, and contributed to data analysis and interpretation and manuscript preparation. S.K. developed the SAP and conducted data analysis, data interpretation and manuscript preparation. R. Schmidt was coordinating investigator and performed data acquisition and study design. P.S. conducted data interpretation and manuscript review for intellectual content. E.K. led immunogenicity assessments, data analysis and interpretation. S.R. performed MRI and DTI evaluation. L. Fialova conducted immunogenicity assessments. M.K. performed data acquisition and manuscript review for intellectual content. N.P.I. conducted immunogenicity assessments. M. Smisek evaluated MRI scans. J.Hanes, E.S., V.P., M.P., J.G., M.C., T.H., P.F. and A.K. performed fluid biomarker analysis. S.S. performed data acquisition and manuscript review for intellectual content. P.K. and M. Samcova undertook safety analysis. J.P. prepared and verified datasets for extended analyses. C.P.G. undertook cognitive assessments. R. Sivak designed the study design and interpreted data. L. Froelich conducted data acquisition and manuscript review for intellectual content. M.F. performed study design, data interpretation, manuscript review for intellectual content. M.R. conducted data acquisition and manuscript review for intellectual content. J. Harrison undertook cognitive assessment and manuscript review for intellectual content. J. Hort undertook data acquisition, manuscript review for intellectual content. M. Otto performed data acquisition, manuscript review for intellectual content. D.T. carried out biomarker prediction via MRI algorithm. M. Ondrus carried out study design, study oversight, SAP, data interpretation and manuscript preparation. B.W. conducted study design, data interpretation, manuscript review for intellectual content. M.N. carried out study design, data analysis and interpretation, manuscript review for intellectual content. N.Z. conducted study design, data analysis and interpretation and manuscript preparation.

Competing interests

All authors affiliated with AXON Neuroscience SE, AXON Neuroscience R&D Services SE or AXON Neuroscience CRM Services SE (P.N., B.K., S.K., E.K., L. Fialova, N.P.-I, M. Smisek, J. Hanes, E. S., A. K., V. P., P. K., M. P., J. G., M. C., P. F., J. P., M. Samcova, C. P.-G., R. Sivak, M. F., M. Ondrus, M. N. and N. Z.) receive salary from the respective companies. T.H. receives salary from AXON Neuroscience R&D services SE. R. Schmidt and S.R. have received personal fees and honoraria for image analyses from AXON Neuroscience. The investigators' institutions have received payments on a per-patient per-visit basis. P. S. has received consultancy/speaker fees (paid to the institution) from AXON, Biogen, People Bio, Roche (Diagnostics) and Novartis Cardiology. He is Principal Investigator of studies with Vivoryon, IONIS, CogRx, AC Immune and Toyama. He serves on the DSMB of Genentech anti-tau study. M. Otto reports personal fees from AXON Neuroscience. The investigator's institution has received payments on a per-patient per-visit basis. B.W. reports personal fees from AXON Neuroscience. The investigator's institution has received payments on a per-patient per-visit basis. J. Hort reports personal fees from AXON Neuroscience. The investigator's institution has received payments on a per-patient per-visit basis. L. Froelich reports personal fees from AXON Neuroscience. The investigator's institution has received payments on a per-patient per-visit basis. M.K.'s institution has received payments on a per-patient per-visit basis. M.R.'s institution has received payments on a per-patient per-visit basis. S.S.'s institution has received payments on a per-patient per-visit basis. J. Harrison reports receipt of personal fees in the past 2 years from AlzeCure, Aptinyx, Astra Zeneca, Athira Therapeutics, AXON Neuroscience, Axovant, Biogen Idec, BlackThornRx, Boehringer Ingelheim, Cerecin, Cognition Therapeutics, Compass Pathways, CRF Health, Curasen, EIP Pharma, Eisai, Eli Lilly, FSV7, G4X Discovery, GfHEU, Heptares, Ki Elements, Lundbeck, Lysosome Therapeutics, MyCognition, Neurocentria, Neurocog, Neurodyn Inc., Neurotrack, Novartis, Nutricia, Probiodrug, Regeneron, Rodin Therapeutics, Samumed, Sanofi, Servier, Signant, Syndesi Therapeutics, Takeda, Vivoryon Therapeutics, vIv Therapeutics and Winterlight Labs. Additionally, he holds stock options in Neurotrack Inc. and is a joint holder of patents with MyCognition Ltd. D.T.'s institution received payments from AXON Neuroscience for image processing during the conduct of the study.

Additional information

Extended data is available for this paper at https://doi.org/10.1038/s43587-021-00070-2.

Supplementary information The online version contains supplementary material available at https://doi.org/10.1038/s43587-021-00070-2.

Correspondence and requests for materials should be addressed to P.N.

Peer review information *Nature Aging* thanks Einar Sigurdsson for their contribution to the peer review of this work.

Reprints and permissions information is available at www.nature.com/reprints.

Publisher's note Springer Nature remains neutral with regard to jurisdictional claims in published maps and institutional affiliations.

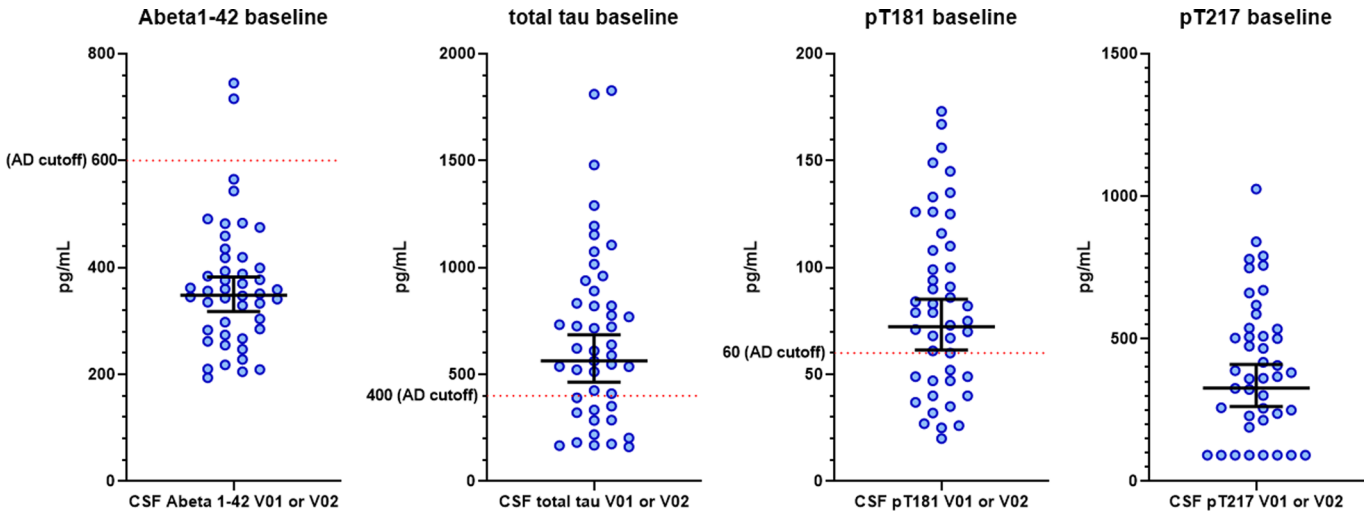

Extended Data Fig. 1 | CSF biomarker baseline values. For pT217, values of 92 pg/mL indicate values < LLOQ. Error bars denote geometric mean and 95% CI. Full analysis set, patients who provided CSF at baseline (n = 46, except for pT217, where 3 patients were not evaluated due to sample depletion).

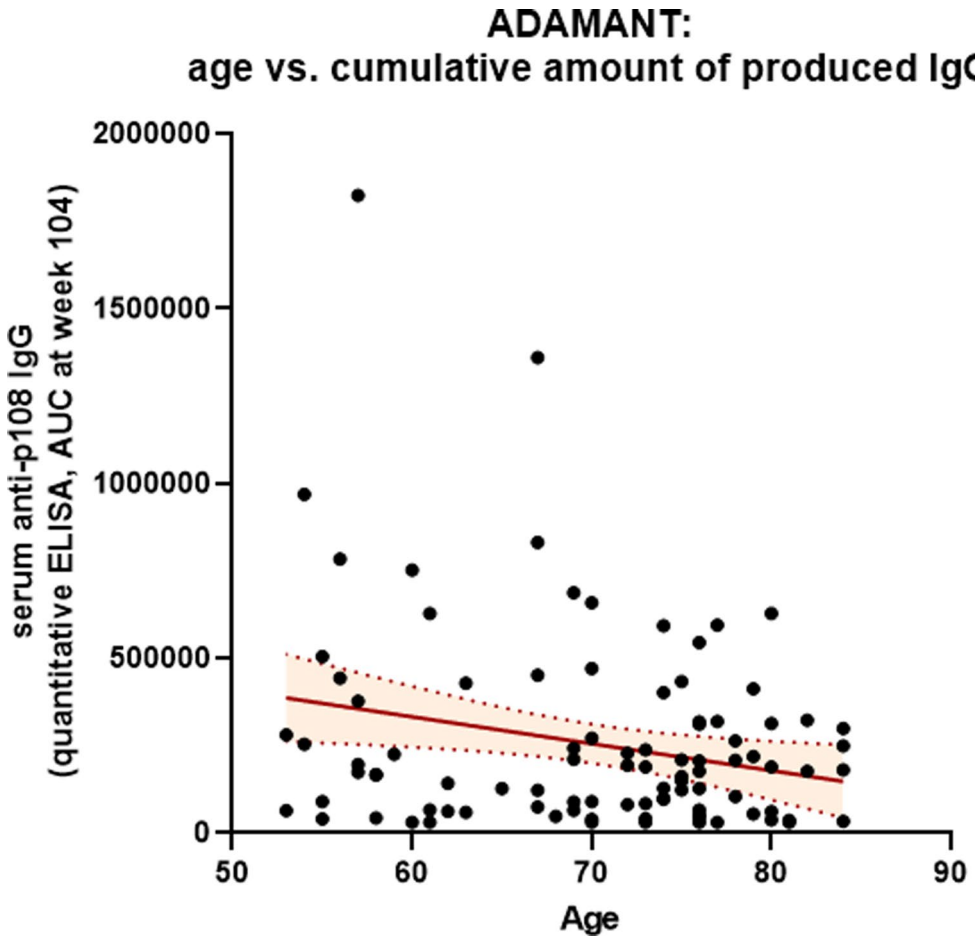

Extended Data Fig. 2 | The association between IgG levels and patient age is fairly loose. Simple linear regression line and 95% confidence bands are shown. FAS, AADvac1-treated completers shown (n = 99, AUC not calculated in one patient due to missing sample). Pearson r −0.2335 (95% CI −0.4119, −0.03785), p = 0.0200.

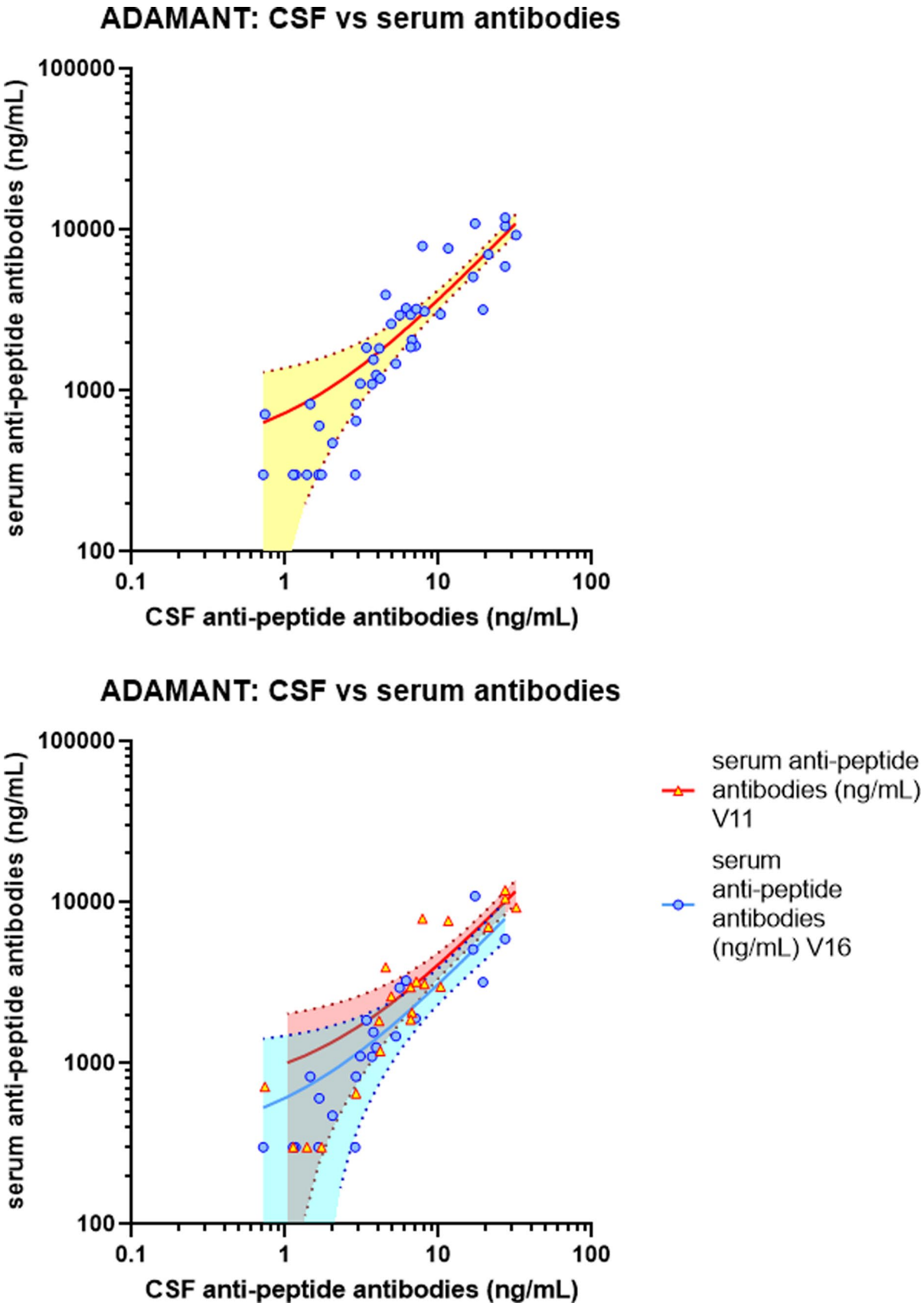

Extended Data Fig. 3 | CSF versus serum antibodies. Overall correlation (above) Spearman r= 0.9351, 95% CI (0.8806, 0.9652), P (two-tailed) <0.0001. Correlation by visit (below): V11 Spearman r = 0.9112, 95% CI (0.7853, 0.9647), p < 0.0001; V16 Spearman r = 0.9341, 95% CI (0.8417, 0.9734), p < 0.0001. Simple linear regression line and 95% confidence bands are shown. FAS, AADvac1-treated patients who provided CSF at V11 and/or V16 (n = 21 and 22, respectively).

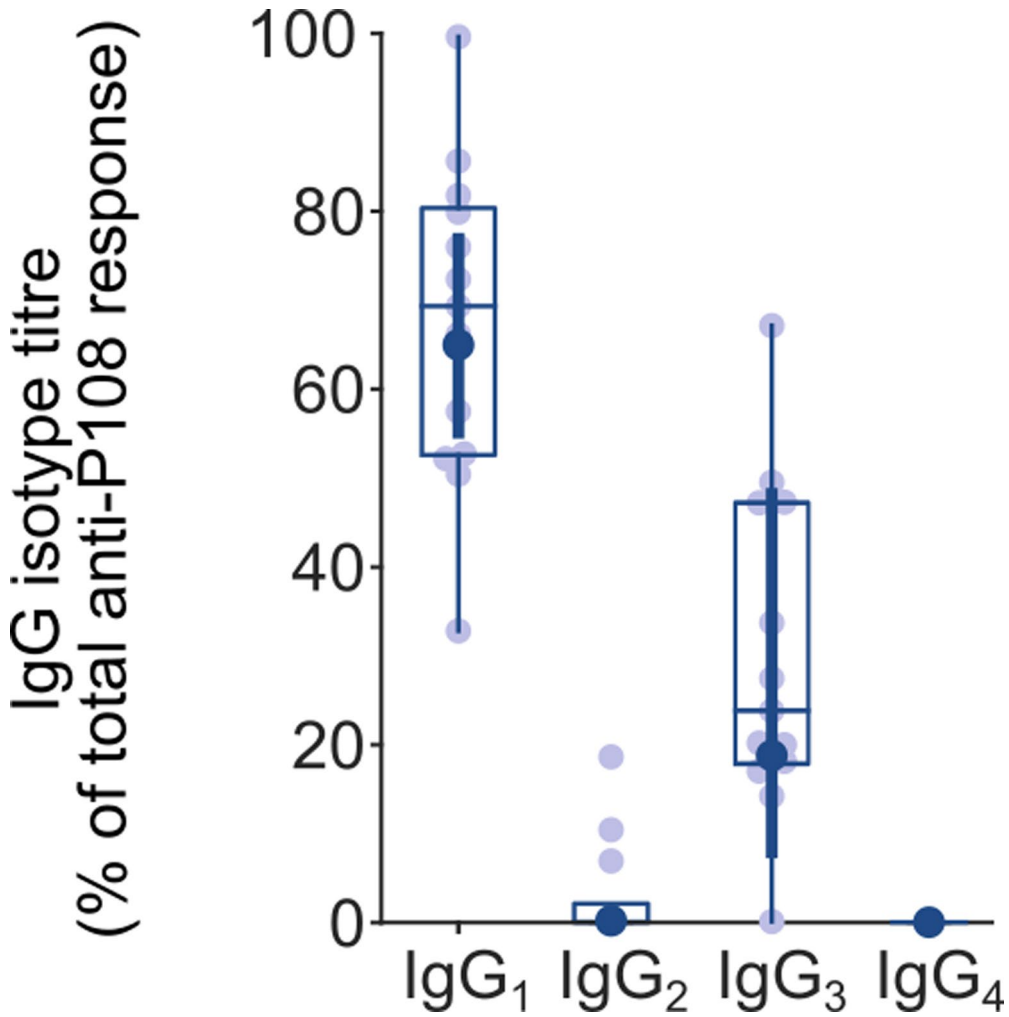

Extended Data Fig. 4 | IgG isotype profile following 4-5 doses of AADvac1. Immunization with AADvac1 predominantly stimulates production antibodies of IgG1 isotype. Values were obtained after 4-5 doses of AADvac1 (n = 13, randomly selected). Thick vertical lines and error bars indicate geometric mean and 95% CI. Boxes indicate median and quartiles. Whiskers indicate 1.5× IQR.

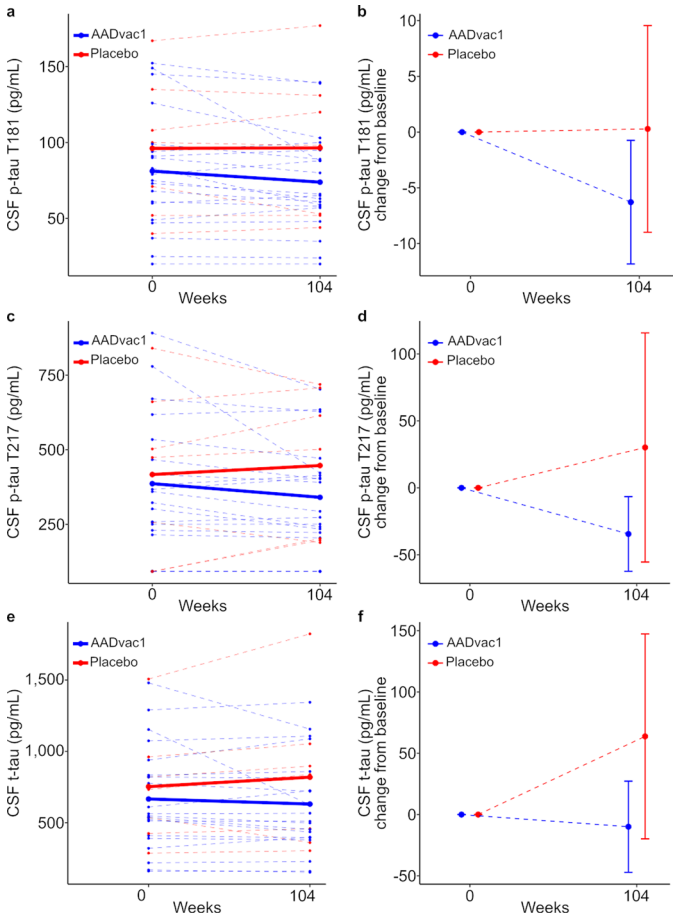

Extended Data Fig. 5 | Changes in CSF tau biomarkers in a subset of placebo- and AADvac1-treated patients across the duration of the trial. Changes in CSF tau biomarkers in a subset of placebo- and AADvac1-treated patients across the duration of the trial Absolute and baseline-adjusted average changes in CSF pT181 phospho-tau (95% CI −17.9080, 1.6567; t-statistic −1.7144; df = 24; p = 0.09935; Cohen's d −0.5749) (a and b), CSF pT217 phospho-tau (95% CI −119.1822, −19.3229; t-statistic −2.8692; df = 23; p = 0.00867; Cohen's d −0.9474) (c and d) and CSF total tau (95% CI −1148.1889, 4.5162; t-statistic −1.9418; df = 24; p = 0.06399; Cohen's d −0.8963) (t-tau; e and f) in a subset of placebo- and AADvac1-treated patients during the 104 weeks of the trial (ANCOVA, adjusted for baseline). On the left are shown the absolute measurements for all individuals (dashed lines) and their mean per group (solid lines). On the right are shown the average baseline-adjusted changes (mean, 95% CI of mean) in the two groups. FAS, AADvac1-treated patients who provided CSF at baseline and end of study shown. pT181, AADvac1 n = 20, placebo n = 7; pT217 phospho-tau, AADvac1 n = 19, placebo n = 7; t-tau, AADvac1 n = 20, placebo n = 7.

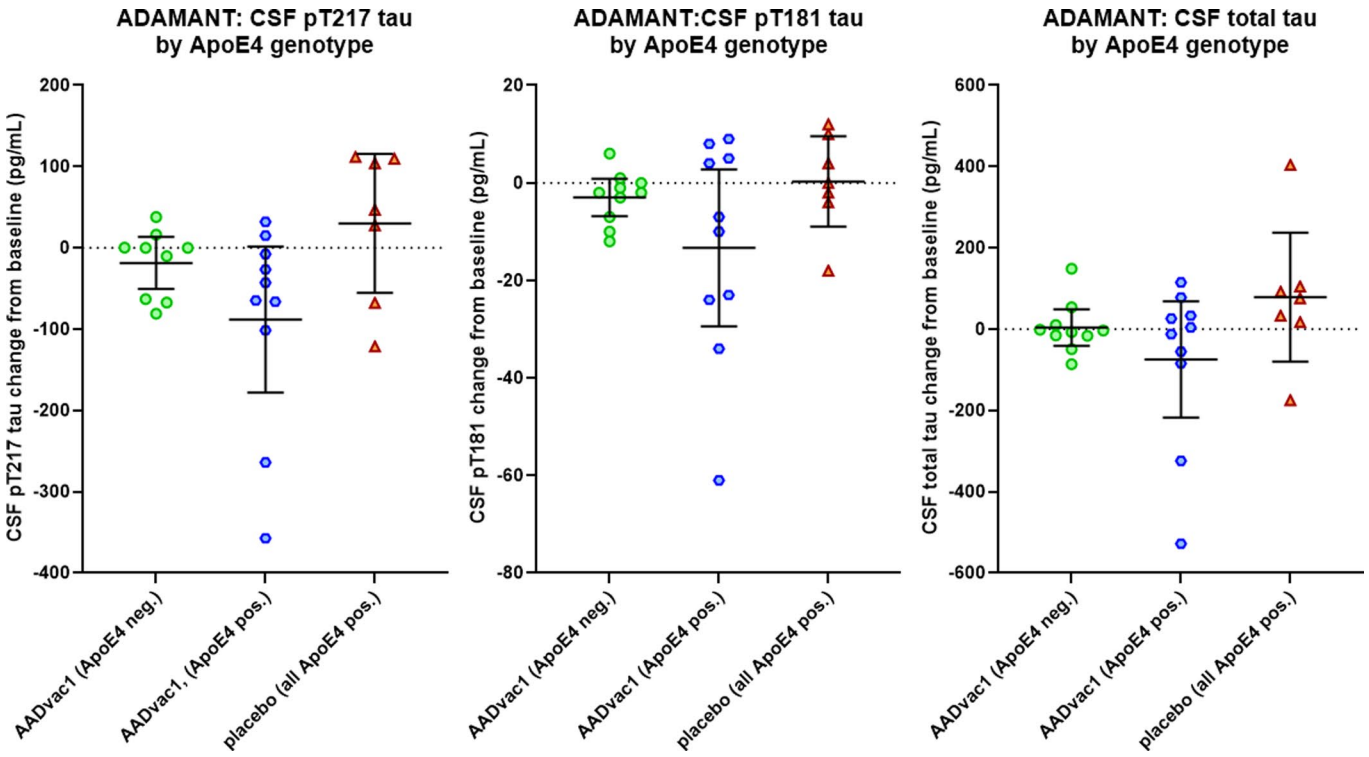

Extended Data Fig. 6 | CSF tau biomarker changes by *APOE4* genotype. Both *APOE4*- and *APOE4* + AADvac1-treated patients contribute to the difference from placebo. Error bars denote mean change and 95% CI of mean. FAS, patients with both baseline and end-of-study values (placebo n = 7, all *APOE4* positive; AADvac1 *APOE4* positive n = 10, *APOE4* negative n = 10 for pT181 and total tau, and n = 9 for pT217 tau).

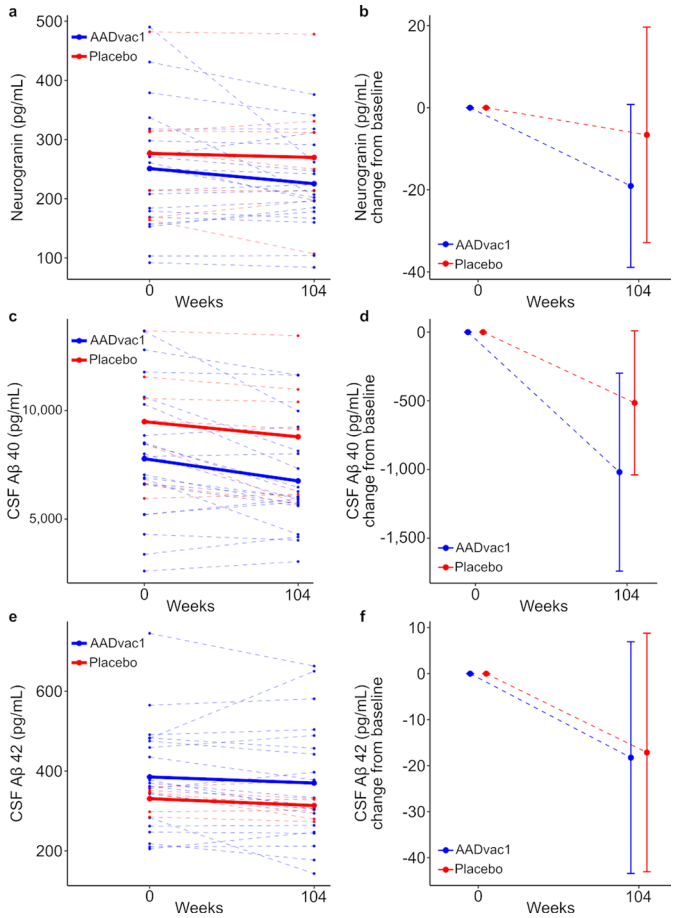

Extended Data Fig. 7 | CSF amyloid and neurogranin. a, Individual patient courses of CSF neurogranin levels. **b**, Both AADvac1 and placebo group showed decrease in neurogranin. (95% CI −48.913, 14.194; t-statistic −1.1355; df = 24; p = 0.26738; Cohen's d −0.3154) Change from baseline (mean, 95% CI of mean shown). **c**, The decrease in CSF Aβ40 in AADvac1 and placebo patients is almost universal. **d**, Both treatment and placebo group showed decrease in Aβ40. (95% CI −2056.972, 280.813; t-statistic −1.5681; df = 24; p = 0.12996; Cohen's d −0.3679) Change from baseline (mean, 95% CI of mean shown). **e**, Individual patient courses of CSF Aβ42 levels. **f**, Both treatment and placebo group showed decrease in Aβ42. (95% CI −47.001, 45.385; t-statistic −0.0361; df = 24; p = 0.97151, Cohen's d −0.0228) Change from baseline (mean, 95% CI of mean shown). FAS, patients who provided baseline and end-of-study CSF samples, AADvac1 n = 20, placebo n = 7.

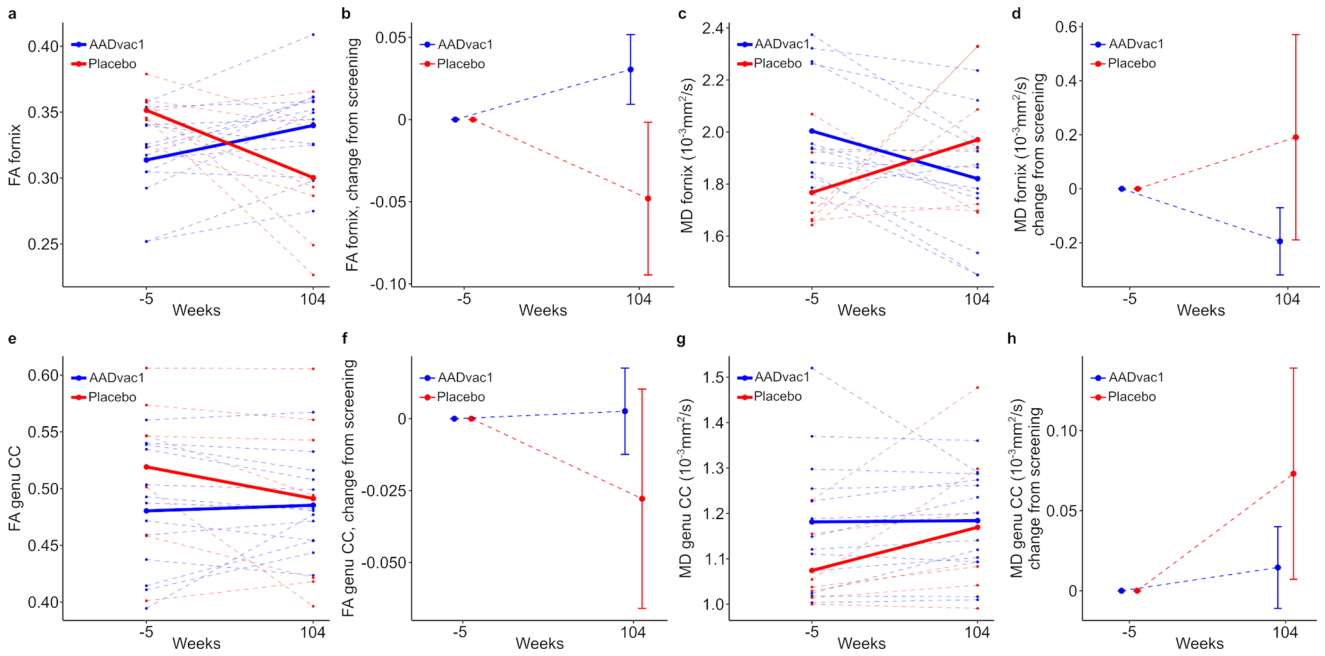

Extended Data Fig. 8 | Effects of AADvac1 treatment on white matter integrity. a–d, Fornix integrity is preserved by treatment **a**, Fractional anisotropy, individual patient courses. Group means shown in bold. **b**, Fractional anisotropy, change from baseline (95% CI 0.0294,0.1277; t-statistic 3.3739; df = 17, p = 0.00361, Cohen's d = 1.9261). **c**, Mean diffusivity, individual patient courses. Group means shown in bold. **d**, Mean diffusivity, change from baseline (95% CI −0.637, 0.041; p = 0.08135, t-statistic −1.8528; df = 17, Cohen's d = −1.3254). **e–h**, Corpus callosum (genu) integrity on AADvac1 vs. placebo treatment. **e**, Fractional anisotropy, individual patient courses. Group means shown in bold. **f**, Fractional anisotropy, change from baseline (95% CI −0.008, 0.055; t-statistic 1.5769; df = 17; p = 0.13324, Cohen's d = 0.9732). **g**, Mean diffusivity, individual patient courses. Group means shown in bold. **h**, Mean diffusivity, change from baseline (95% CI −0.11, 0.005; t-statistic −1.9262; df = 17; p = 0.07097; Cohen's d −1.0913). FAS, patients who had both baseline and end of study DTI sequences (AADvac1 n = 13, placebo n = 7). Panels b,d,f,h show mean and 95% CI of mean change.

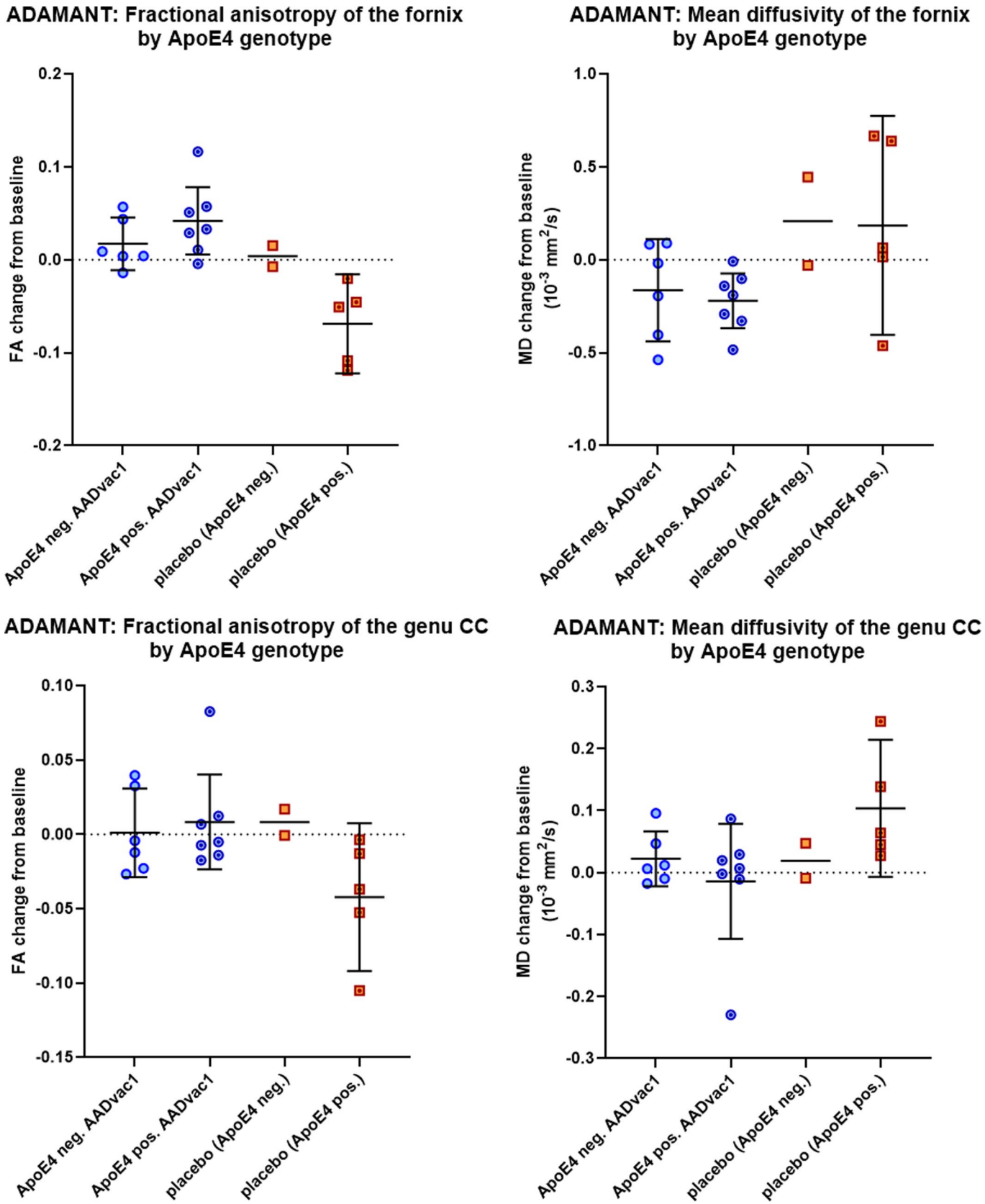

Extended Data Fig. 9 | DTI changes by *APOE4* genotype. Both *APOE4*– and *APOE4* + AADvac1-treated patients contribute to the difference from placebo. Error bars denote mean change and 95% CI of mean (for *APOE4*– placebo, only the mean is shown). FAS, patients who had DTI sequences at baseline and end of study (n = 20). AADvac1: *APOE4* neg. n = 6, *APOE4* pos. n = 7. Placebo: *APOE4* neg. n = 2, *APOE4* pos. n = 5.

nature research

Corresponding author(s): Petr Novak, MD, PhD

Last updated by author(s): Apr 12, 2021

Reporting Summary

Nature Research wishes to improve the reproducibility of the work that we publish. This form provides structure for consistency and transparency in reporting. For further information on Nature Research policies, see Authors & Referees and the Editorial Policy Checklist.

Statistics

For all statistical analyses, confirm that the following items are present in the figure legend, table legend, main text, or Methods section.

n/a	Confirmed	
☐	☒	The exact sample size (*n*) for each experimental group/condition, given as a discrete number and unit of measurement
☐	☒	A statement on whether measurements were taken from distinct samples or whether the same sample was measured repeatedly
☐	☒	The statistical test(s) used AND whether they are one- or two-sided *Only common tests should be described solely by name; describe more complex techniques in the Methods section.*
☐	☒	A description of all covariates tested
☐	☒	A description of any assumptions or corrections, such as tests of normality and adjustment for multiple comparisons
☐	☒	A full description of the statistical parameters including central tendency (e.g. means) or other basic estimates (e.g. regression coefficient) AND variation (e.g. standard deviation) or associated estimates of uncertainty (e.g. confidence intervals)
☐	☒	For null hypothesis testing, the test statistic (e.g. *F*, *t*, *r*) with confidence intervals, effect sizes, degrees of freedom and *P* value noted *Give P values as exact values whenever suitable.*
☒	☐	For Bayesian analysis, information on the choice of priors and Markov chain Monte Carlo settings
☒	☐	For hierarchical and complex designs, identification of the appropriate level for tests and full reporting of outcomes
☐	☒	Estimates of effect sizes (e.g. Cohen's *d*, Pearson's *r*), indicating how they were calculated

Our web collection on statistics for biologists contains articles on many of the points above.

Software and code

Policy information about availability of computer code

Data collection	• Medidata RAVE Electronic Data Capture system, used as electronic case report forms for collection and management of clinical data • Medavante Virgil, the eSource platform, provides digital clinical outcome assessments and data management for clinical scales outcomes • Cogstate Datapoint Software System, a secure online portal, enabling efficient data collection and storage for ongoing review of data quality • Cogstate Box system served for uploading documents and recordings produced by investigational sites • PPD Preclarus central laboratory database for recording and management of central laboratory data • InfoMED LabIS, a laboratory information system enabling lab data collection and storage • IXICO's online image data management system TrialTracker, a web-based platform designed to facilitate the live tracking, upload, and reporting of imaging data for MRI and FDG PET outcomes • eRT EXPERT Clinical Data Management System for acquisition, measurement and cardiology review and all associated processes • Cenduit's Interactive Response Technology providing Interactive Web Response System for allocation and tracking of treatment of study subjects • Simoa HD-1 instrument software v1.5 was used to evaluate neurofilament light chain protein and pT217 tau levels in the respective assays. • SIENA 2.6 (part of FSL, FMRIB Oxford) and Freesurfer v6.0 were used for volumetric analyses. FSL 6.0 (FMRIB Software Library, Oxford) was used to evaluate diffusion-weighted scans.
Data analysis	We performed the statistical analyses using the R programming environment version 4.0.5 (R Development Core Team 2020; R: A language and environment for statistical computing. R Foundation for Statistical Computing, Vienna, Austria. URL https://www.R-project.org/) and GraphPad Prism version 8.4.3 (GraphPad software, CA, USA). For ANCOVA we used SAS software (SAS(R) Proprietary Software 9.4 (TS1M5)).

For manuscripts utilizing custom algorithms or software that are central to the research but not yet described in published literature, software must be made available to editors/reviewers. We strongly encourage code deposition in a community repository (e.g. GitHub). See the Nature Research guidelines for submitting code & software for further information.

Data

Policy information about availability of data

All manuscripts must include a data availability statement. This statement should provide the following information, where applicable:

- Accession codes, unique identifiers, or web links for publicly available datasets
- A list of figures that have associated raw data
- A description of any restrictions on data availability

The data that support the findings of this study are available from the corresponding author PN upon reasonable request.

Field-specific reporting

Please select the one below that is the best fit for your research. If you are not sure, read the appropriate sections before making your selection.

☒ Life sciences ☐ Behavioural & social sciences ☐ Ecological, evolutionary & environmental sciences

For a reference copy of the document with all sections, see nature.com/documents/nr-reporting-summary-flat.pdf

Life sciences study design

All studies must disclose on these points even when the disclosure is negative.

Sample size	An overall dropout rate of 25% was assumed. Sample sizes were increased to correct for dropout. Dropouts were not to be replaced. For the primary objective (safety assessment): The study was powered to detect an AE with an incidence of 7% and higher. At least 83 subjects on AADvac1 treatment were required to complete the study to show an AE incidence of 7% and higher as statistically significant with a power of 0.80 at the significance level of 0.05, using a one-sided one-sample Wald Z-test. Correcting for 25% dropout, at least 111 subjects would need to be enrolled and randomised in the AADvac1 arm. Given a 3:2 AADvac1 to placebo allocation, at least 55 subjects on placebo treatment were required to complete the study. Correcting for 25% dropout and given a 3:2 AADvac1 to placebo allocation, at least 74 subjects needed to be enrolled and randomised in the placebo arm. With 111 patients enrolled in the AADvac1 group and 83 patients on AADvac1 treatment expected to complete the 2-year trial, 194 patient-years of on-treatment safety data were to be generated (assuming linear dropout). Given this data set, the study had a > 95% chance to observe at least one occurrence of hypothetical AEs with a true annual incidence of 1:65 or higher. A non-inferiority post-hoc power calculation was also undertaken. With a 15% non-inferiority margin, a trial with 97 subjects on AADvac1 and 65 on placebo (162 patients in total) has 80% power in a one-sided non-inferiority test at the significance level of 0.1, to demonstrate non-inferiority of AADvac1 to placebo with respect to incidence of AEs if AADvac1 has a 7% higher incidence of AEs compared to placebo; using a two-sample Wald z-test with adjustment according to [Agresti, A. and B. Caffo, Simple and Effective Confidence Intervals for Proportions and Differences of Proportions Result from Adding Two Successes and Two Failures. The American Statistician, 2000. 54(4): p. 280-288.] (H0: the incidence of AEs in AADvac1 minus Placebo >= 0.15; H1: the incidence of AEs in AADvac1 minus Placebo < 0.15). For the secondary clinical and cognitive endpoints: With 138 patients targeted to complete the study, the ADAMANT trial was powered to detect an effect size of 0.5 with a power of 0.80 at a two-tailed significance level of 0.05 (taking the 3:2 randomisation ratio into account). No sample size calculations were done for exploratory endpoints. (The study size was set primarily according to the safety analysis, and informed by the power calculations for secondary clinical endpoints. No sample size calculation was done for exploratory and research endpoints; the intent was simply to analyze whatever the resulting amount of data would be. For many novel endpoints, e.g., NfL, pT217 tau or DTI, a sample size calculation was not feasible because of the paucity of data on longitudinal change of these endpoints over time – especially considering the study was designed in 2015).
Data exclusions	One site (#31802) was excluded from analysis due to severe misconduct identified during a for-cause audit (data manipulation, deficiencies in data quality and integrity, issues with attributability of data, deficiencies in safety reporting). Data from this site are not included in any analyses.
Replication	For immunogenicity, antibody response measurements were performed in duplicate. For fluid biomarkers, all measurements were performed in duplicate. Cognitive and functional assessments are inherently non-replicable. Patients were assessed every 3 months over the course of the study to evaluate the consistency of assessment. MRIs were subjected to quality control, and scans that failed quality control either repeated, or excluded from analysis. Attempts are replication were successful. Where the duplicate analyses did not align, samples were re-assessed.
Randomization	Patients were randomised via an interactive web-based response system (IWRS). The AADvac1: placebo randomisation ratio was 3:2. The randomisation block size was 10.
Blinding	AADvac1 and placebo vials were identical in appearance. Each vial was labelled with a unique identifier code assigned by an independent vendor, and the specific vial to be administered to a given patient at a given visit was allocated prior to administration by the interactive web-

based response system. Patients, caregivers, investigators, outcome assessors, and all other personnel involved in trial conduct were blinded to treatment allocation.

Reporting for specific materials, systems and methods

We require information from authors about some types of materials, experimental systems and methods used in many studies. Here, indicate whether each material, system or method listed is relevant to your study. If you are not sure if a list item applies to your research, read the appropriate section before selecting a response.

Materials & experimental systems

n/a	Involved in the study
☐	☒ Antibodies
☒	☐ Eukaryotic cell lines
☒	☐ Palaeontology
☒	☐ Animals and other organisms
☐	☒ Human research participants
☐	☒ Clinical data

Methods

n/a	Involved in the study
☒	☐ ChIP-seq
☒	☐ Flow cytometry
☐	☒ MRI-based neuroimaging

Antibodies

Antibodies used

See Methods section "Antibodies used in this study"
* Humanized Mab AX004, targeting the tau assembly-regulating domains in MTBR region, generated by AXON Neuroscience, patent WO2016079597A1 [Weisova, P., et al., Therapeutic antibody targeting microtubule-binding domain prevents neuronal internalization of extracellular tau via masking neuron surface proteoglycans. Acta Neuropathol Commun, 2019., Zilkova, M., et al., Humanized Tau Antibodies Promote Tau Uptake By Human Microglia Without Any Increase Of Inflammation. Acta Neuropathologica Communications, 2020.];
* mouse DC2E7, targeting tau phospho-threonine pT217, generated by AXON Neuroscience, patent WO 2019/186276 A2. 2019-10-03 [Hanes, J., et al., Novel Immunoassay Detecting p-Tau Thr217 Distinguishes Alzheimer's Disease from Other Dementias. . Neurology, 2020.];
* mouse DC2E2, targeting tau 164-174, generated by AXON Neuroscience, patent WO 2019/186276 A2. 2019-10-03 [Hanes, J., et al., Novel Immunoassay Detecting p-Tau Thr217 Distinguishes Alzheimer's Disease from Other Dementias. . Neurology, 2020.]; .
* Goat anti-Human IgG (H+L); Secondary Antibody, HRP conjugate, Catalogue Number: 31410, Lot Number: QE2020434; (Thermo Fisher Scientific, Rockford, IL 61105, USA)
* Mouse anti-Human IgG1 heavy Chain Secondary Antibody, HRP conjugate, Catalogue Number: MH1715, Lot Number: 1870367; Clone: HP6070; (Thermo Fisher Scientific, Rockford, IL 61105, USA)
* Mouse anti-Human IgG2 heavy Chain Secondary Antibody, HRP conjugate, Catalogue Number: MH 1722, Lot Number: 1873763, Clone: HP6014; (Thermo Fisher Scientific, Rockford, IL 61105, USA)
* Mouse anti-Human IgG3 heavy Chain Secondary Antibody, HRP conjugate, Catalogue Number: 05-3620, Lot Number: QD215257, Clone: HP6047; (Thermo Fisher Scientific, Rockford, IL 61105, USA)
* Mouse anti-Human IgG4 heavy Chain Secondary Antibody, HRP conjugate Catalogue Number: MH1742, Lot Number: 1831840, Clone: HP6023 (Thermo Fisher Scientific, Rockford, IL 61105, USA)

Validation

See Methods section "Antibodies used in this study"
Primary antibodies: humanized Mab AX004, specific to the tau assembly-regulating domains in MTBR region, validated using tau protein in ELISA, published in [Weisova, P., et al., Therapeutic antibody targeting microtubule-binding domain prevents neuronal internalization of extracellular tau via masking neuron surface proteoglycans. Acta Neuropathol Commun, 2019., Zilkova, M., et al., Humanized Tau Antibodies Promote Tau Uptake By Human Microglia Without Any Increase Of Inflammation. Acta Neuropathologica Communications, 2020.] and patented in WO2016079597A1; mouse DC2E7, specific to tau phospho-threonine pT217; mouse DC2E2, specific to tau protein targeting tau epitope 164-174, both validated in [Hanes, J., et al., Novel Immunoassay Detecting p-Tau Thr217 Distinguishes Alzheimer's Disease from Other Dementias. . Neurology, 2020.] and patented in WO 2019/186276 A2. 2019-10-03;
Secondary antibodies: all secondary antibodies were validated by each respective manufacturer, as per the pertinent DataSheets.

Human research participants

Policy information about studies involving human research participants

Population characteristics

The study enrolled patients of both sexes aged 50-85 with a diagnosis of Alzheimer's disease dementia according to the 2011 NIA-AA criteria (McKhann et al., 2011), with evidence of medial temporal lobe atrophy (Scheltens score 2+) and/or an AD amyloid and tau biomarker profile in the CSF. Patients were required to be on standard acetylcholinesterase inhibitor therapy; concomitant therapy with memantine was allowed.
Baseline demographic characteristics of the population are listed in Table 1 in the article.

Recruitment

The investigational sites, hospitals and outpatient clinics, pre-selected the potential study participants from their own databases and in some instances based on references. After providing informed consent, patients underwent the screening procedures set

by the study protocol, such as assessments of clinical status including clinical scales, blood tests and MRI, and optionally CSF biomarkers. After all required data for a specific patients was collected, the Investigator and the Sponsor evaluated its consistency with the Inclusion and Exclusion criteria. Only after the eligibility was centrally confirmed the patient was enrolled and randomized to one of the treatment arms. No waivers to Inclusion and Exclusion criteria were granted. No selection biases were identified.

Ethics oversight

Ethikkommission der Medizinischen Universitat Graz /
Ethics Committee of the Medical University Graz
Auenbruggerplatz 2, 3. OG
8036 Graz
Austria

Eticka komise Fakultni nemocnice v Motole
Fakultní nemocnice v Motole
V úvalu 84
150 06 Praha 5 – Motol
Czech Republic

Ethik-Kommission II der Universität Heidelberg Universitätsklinikum Mannheim
Haus 42, Ebene 3
Theodor-Kutzer-Ufer 1-3
68167 Mannheim
Germany

Eticka komisia Univerzitnej nemocnice L. Pasteura Kosice
Rastislavova 43
041 90 Košice
Slovakia

National Medical Ethics Committee,
Ministry of Health,
Komisja Republike Slovenije,
Za medicinsko etiko,
Stefanova 5,
SI-1000 Ljubljana,
Slovenia

Regionala etikprövningsnämnden i Stockholm
Karolinska Institutet/Solna
Widerstromska huset,
Tomtebodavägen 18A, plan 3
171 65 Solna,
Sweden

National Bioethics Committee for Medicine and Medical Devices
Comisia Nationala de Bioetica a Medicamentului si a Dispozitivelor Medicale Sos. Stefan cel Mare nr. 19-21
020125, Sector 2, Bucuresti,
Romania

Komisja Bioetyczna przy Bydgoskiej Izbie Lekarskiej
ul. Powstańców Warszawy 11
85-681 Bydgoszcz
Poland

AGES Medizinmarktaufsicht
Bundesamt fur Sicherheit im
Gesundheitswesen
Traisengasse 5
1200 Wien
Austria

Statni ustav pro kontrolu leciv, SUKL
Srobarova 48
100 41 Praha 10
Czech Republic

Paul Ehrlich Institut (PEI)
Paul-Ehrlich-Strase 51-59
D-63225 Langen
Germany

Urząd Rejestracji Produktow Leczniczych,
Wyrobow Medycznych i Produktow
Biobojczych
181 C Jerozolimskie Avenue

02-222 Warsaw
Poland

Agentia Națională a Medicamentului și
Dispozitivelor Medicale (NAMMD)
Str. Av, Sănătescu nr. 48, sector 1
011478 Bucureşti
Romania

Statny ustav pre kontrolu lieciv – SUKL
Sekcia klinickeho skusania liekov a farmakovigilancie
Kvetna 11
825 08 Bratislava 26
Slovakia

Lakemedelsverket (MPA)
P.O. Box 26
SE-751 03
Uppsala
Sweden

Javna agencija RS za zdravila in medicinske
pripomocke (JAZMP)
Slovenceva ulica 22
1000 Ljubljana
Slovenia

Note that full information on the approval of the study protocol must also be provided in the manuscript.

Clinical data

Policy information about clinical studies

All manuscripts should comply with the ICMJE guidelines for publication of clinical research and a completed CONSORT checklist must be included with all submissions.

Clinical trial registration	Study registration: EudraCT 2015-000630-30; NCT02579252.
Study protocol	The study protocol will be uploaded with the submission.
Data collection	The data included in the analyses were collected in the period from the first visit of the first patient screened on the 10th of May 2016 until the end-of-study visit of the last patient which took place on the 25th of May 2019. The first subject was randomised 16th June 2016. The last safety follow-up was on 25 June 2019. The data were collected through electronic data capture systems at investigation sites and through centralized vendors databases such as MRI readings and volumetry, DTI data, FDG PET data, laboratory results and ECG results.
Outcomes	Full statistical methodology is provided in the supplement.

Magnetic resonance imaging

Experimental design

Design type	Resting state.
Design specifications	140 volumes, repetition time = 3 s, total duration = 7 min
Behavioral performance measures	No behavioral performance measures were used.

Acquisition

Imaging type(s)	structural and diffusion
Field strength	3T
Sequence & imaging parameters	T2 FLAIR (TR/TI/TE = 10,000/2,600/100-120 ms, slice thickness = 5mm, slice gap = 0 mm, field of view = 240mm, matrix=256x256); T2 TSE (TR/TE = 2,000-4,000/80-120 ms, slice thickness = 5mm, slice gap = 0 mm, field of view = 240mm, matrix=256x256); T2* gradient echo (TR/TE= 600-700/20 ms, flip angle = 20°, slice thickness = 5mm, slice gap = 0 mm, field of view = 240mm, matrix=256x256); T1W 3D (MPRAGE or T1-TFE, 1mm isotropic resolution with whole brain coverage)
Area of acquisition	whole brain

Diffusion MRI ☒ Used ☐ Not used

Parameters: TR = 7s, TE = 80–100 ms, 41 diffusion directions with b = 1000 s/mm2, 5 repeats of b=0 s/mm2, 2.7 mm isotropic resolution, single shot echo planar imaging readout with SENSE/GRAPPA factor of 2-3.

Preprocessing

Preprocessing software: Whole brain volume loss was calculated with SIENA 2.6 (part of FSL, FMRIB Oxford); Regional atrophy was assessed with the longitudinal Stream of FreeSurfer version 6 (Fischl B, Neuroimage 2012;62:774).

Normalization: 3D T1 scans were normalized by non-linear registration to a template. Diffusion weighted scan were registered through the corresponding 3D T1 scans and by using the b0 scan as reference. The obtained transformation matrix then was applied to the entire diffusion weighted (b=1000 s/mm2) series.

Normalization template: MNI305

Noise and artifact removal: All scans that were affected by noise and motion artefacts were repeated or excluded from analysis

Volume censoring: not done

Statistical modeling & inference

Model type and settings: Following preprocessing (motion correction, spatial smoothing, temporal high-pass filtering), a temporal-concatenation independent component analysis approach was used to calculate group-level components of the resting state networks. The following networks have been assessed: Default mode network, the right fronto-parietal network, the left fronto-parietal network, and the salience network. Based on a general linear model, a dual regression approach was applied to obtain time courses of these networks for each patient.

Effect(s) tested: Non-parametric testing for temporal differences and for between-group effects (placebo versus verum).

Specify type of analysis: ☐ Whole brain ☐ ROI-based ☒ Both

Anatomical location(s): Anatomical locations were determined from automated labeling with FreeSurfer

Statistic type for inference (See Eklund et al. 2016): Not applicable for the employed paradigms.

Correction: Correction for multiple comparisons with FDR

Models & analysis

n/a	Involved in the study
☒	☐ Functional and/or effective connectivity
☒	☐ Graph analysis
☒	☐ Multivariate modeling or predictive analysis